Chapter II

Experimental

2.1 Construction and Installation of Experimental Set Up

To avoid the distortion of the magnetic field by the apparatus, nonmagnetic materials such as brass or aluminium had to be used for the construction of the experimental set up. The set up included the sample chamber with heater and temperature measurement device, the polarizer holder, the light source, and a supporting shaft for mounting the sample chamber, the microscope, the camera, the polarizer and the light source in the gap of an electromagnet. The set up had to be designed and arranged in such a way that the short focal length microscope could focus on the sample placed in the middle of the pole gap of the electromagnet with the pole pieces having the least separation possible so that high field could be achieved. The schematic of the set up is shown in Fig. 9 .

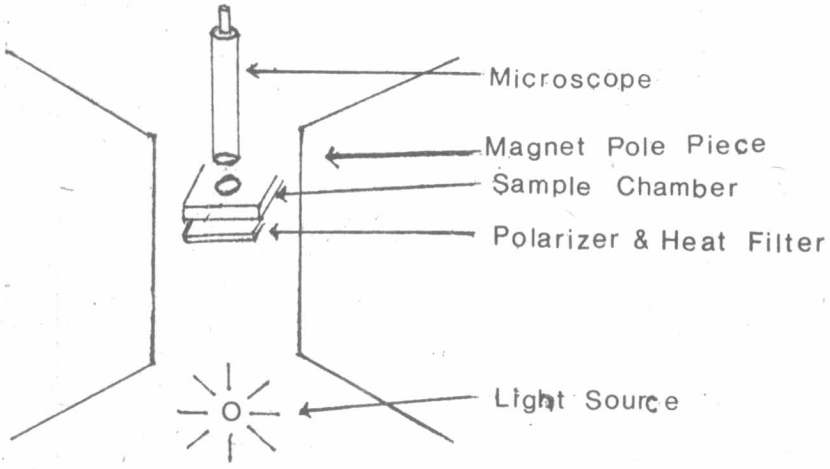

Fig. 9 Schematic diagram of the experimental set up installed in the magnet

2.1.1 The sample chamber

The first sample chamber was made by drilling out a hollow cylinder brass pipe. The inner diameter was 3 centimeters and its length was 2.9 centimeters. The wall was 0.25 centimeter thick. The heater wire was wound on a smaller brass cylinder and placed inside the bigger brass sample chamber. High specific resistance nichrom wire was used as the heater wire. Several hundred turns of the wire were needed to obtain the heating power required with a low electric current.

A thin mica sheet was used as electrical insulator between the heater and the brass sample chamber wall. Two layers of nichrom wire were used. The layers of heater wire were insulated by mica sheets. The two layers of wire consisted of equal numbers of turns of wire wound in opposite directions so that the magnetic field generated by one layer of the heater wire was exactly cancelled by that generated by the second layer of heater wire.

A glass slide was cut and milled by rotating grinding stone into a circular disc which fitted into the inner cylindrical pipe. It was fixed in the middle of the sample chamber. This glass disc became the hot stage for placing samples for observation. The sample chamber was enclosed at both ends with brass caps fitted with glass window for light transmission and observation. The tip of the pair of the chromel-alumel thermocouple wires was attached to the inside of the inner brass cylinder near the glass hot stage. The thermocouple output was measured with a PAR 135 electrometer. The schematic diagram of the sample chamber is shown in Fig. 10.

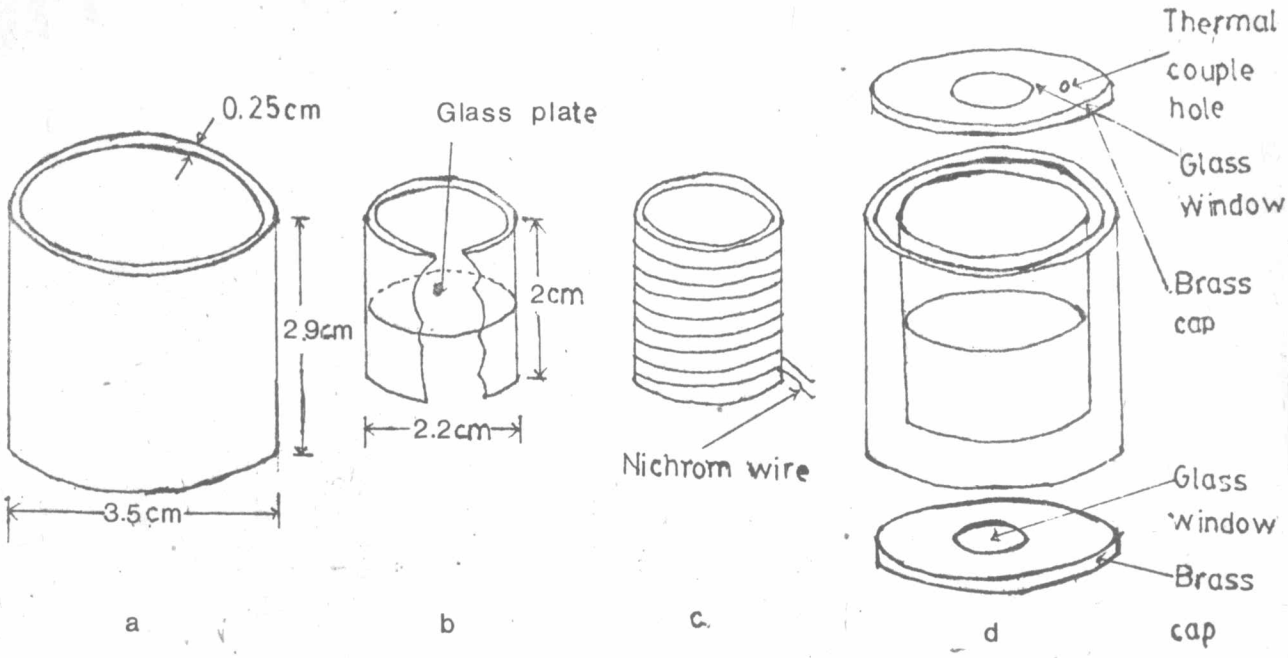

Fig. 10 Schematic diagram of the sample chamber

a) The outer brass cylindrical pipe

b) The inner brass cylindrical pipe with circular glass disc hot stage

c) The nichrom heater wire wound on the inner cylinder

d) Diagram showing all parts of the sample chamber

A testing of the sample chamber was carried out to examine the heating characteristics, magnetic field generated by the heater wire and the period of time needed to get steady temperatures. The sample chamber with heater wire resistance of 750 ohms was supplied with 75 volts dc from a regulated power supply. The thermocouple read a steady temperature of $155 \pm 2^{\circ}C$ in about 30 minutes. Other values of heater wire currents yielded about the same heating time constant. The magnetic field generated by the heater wire could not be detected by a small compass held near the sample chamber.

After a period of use, it was realized that there were many disadvantages with this first sample chamber such as the long heating time required because the chamber contained no cooling system. A second sample chamber was therefore constructed.

The second sample chamber was made of aluminium sheet containing the automatic heating and temperature sensing unit of a commerical hot stage, Mettler model FP 52. To provide cooling in the sample chamber, an air pump was used. The schematic diagram of the second sample chamber is shown in Fig. 11a, and a photograph is shown in Fig. 11b.

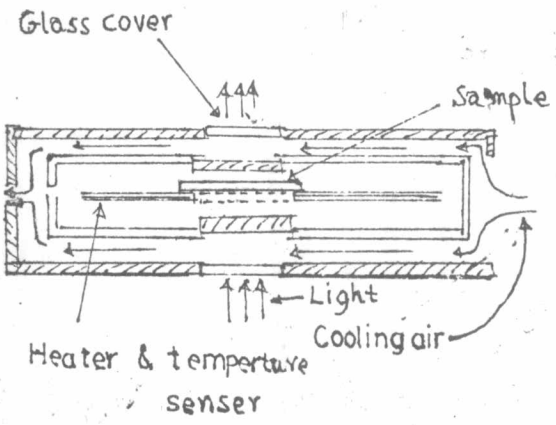

a)

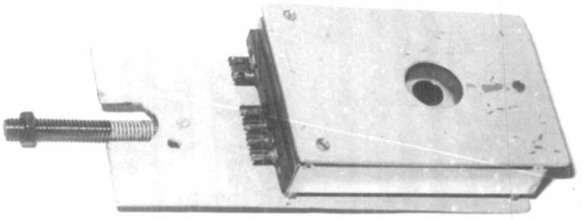

b)

Fig. 11 a) The side view of the second sample chamber

b) The photograph of the second sample chamber

The imprecision of the temperature of the Mettler unit is $\pm$ 0.1 ^{o}C within the range 30^{o}C to 100^{o}C and $\pm$ 0.2^{o}C within the range 100^{o}C to 200^{o}C with the 0.2^{o}C/min heating rate and under isothermal conditions. The counter shows readings in steps of 0.1^{o}C.

2.1.2 Microscopy and photography

A microscope with brass tubing was used. An eyepiece with a graduated scale was used for the pitch measurements which were done with a 10x Keller eyepiece with movable cross wires and a micrometer. A standard micrometer scale by E. LEITZ was used for the calibration of the eyepiece-micrometer. A camera could be mounted on the microscope when photographs were to be taken.

2.2 Sample Preparation

The samples were thin films on glass slides covered by glass slip. The slides were cut into circular shape just big enough to fit on to the circular hot stage in the sample chamber.

2.2.1 Weighing

Since very low concentrations ($\leq$ 0.2 %) of cholesteric were to be studied, and, because liquid crystals are expensive and consequently only small quantities of the materials were available for experiment, accurate weighing of liquid crystals for preparing the samples was somewhat of a problem. A commerical electric balance by Mettler was used. The balance has a continuous range of reading from 0.0001 gram to 10 gram with decade

range switchs. The accuracy of the balance was $\pm$ 0.0001 gram. Error in cholesteric concentration of the sample could be one significant source of error in our data.

2.2.2 Mixing of cholesteric with nematic

To ensure good mixing of the nematic with the cholesteric, the weighed mixture was first ground together into powder. The mixed powder was placed in a test tube and heated in an oil bath until an isotropic solution was obtained. The test tube containing the solution was then vigorously shaken for 15-20 seconds before it was cooled down rapidly in cool water. This process was repeated several times until good mixing was obtained.

2.2.3 Rubbing of slides

The Châtelain technique[27] for rubbing glass slides for the sample was employed. A small piece of slide was constrained between two long glass slides and the smaller piece was rubbed on drawing paper about 50 times in only one direction. After that the rubbed slide was cleaned with a sheet of lenspaper.

2.2.4 Spacer and sample thickness

After the liquid crystal sample was placed on the rubbed slide, it was covered with a glass slip placed over spacers. The thickness of the

---

[27] P. Châtelain, Bull. Soc - Franc - Mineral. 60(1937), 300.

sample was taken to be simply the thickness of the spacers. Mica sheets in thickness of 50, 75, 100, 125, 150, 200, 250 and 300 μm were used as spacers. These mica sheets were cleaved off a thicker pack with a razor. For thinner samples, mylar sheets in 25 μm thickness were used. However, there were always wrinkles in the mylar sheets owing to their being folded for mailing. The wrinkles were removed by heat by bringing the sheet to within 6 inches of a 150watts incandescent bulb. The thickness of the mica spacers was measured with a micrometer having an accuracy of $\pm$ 2 μm.

2.3 Measurements

2.3.1 Temperature dependence of the cholesteric pitch

The cholesteric pitch is shown in photographs in Fig.12. The systems of PAA/CP (0.2, 0.3, 0.4, 0.5 and 0.75 %) were studied for the effect of temperature on the helical pitch in the temperature range 90^{o} - 132^{o}C. The isotropic transition temperature of PAA is 135^{o}C.

It was found that, within the accuracy of the measurement, the pitch does not vary with temperature in this temperature range.

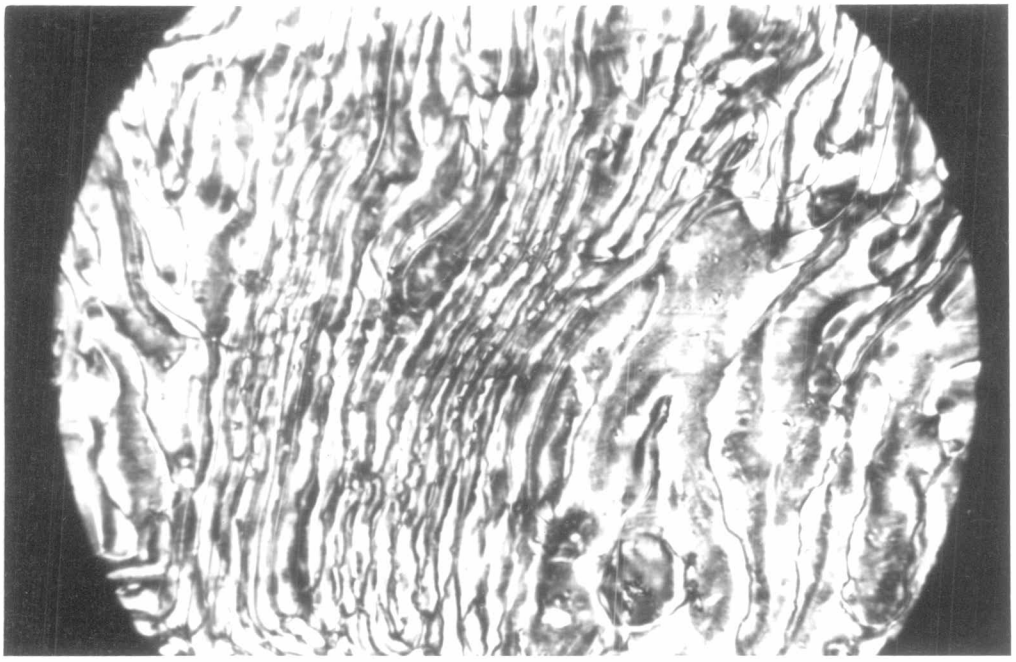

Fig. 12 PAA doped with 0.5 % CP showing the cholesteric pitch. The pitch is approximately 26 μm.

a) T = 100°C (supercool state)

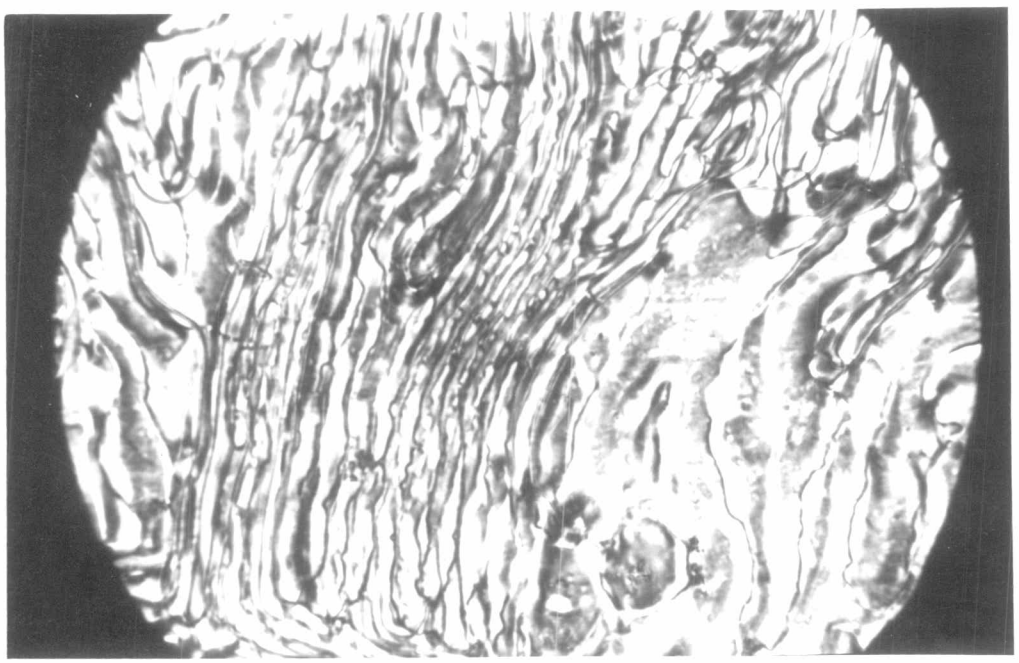

b) T = 118.1°C (mesophase)

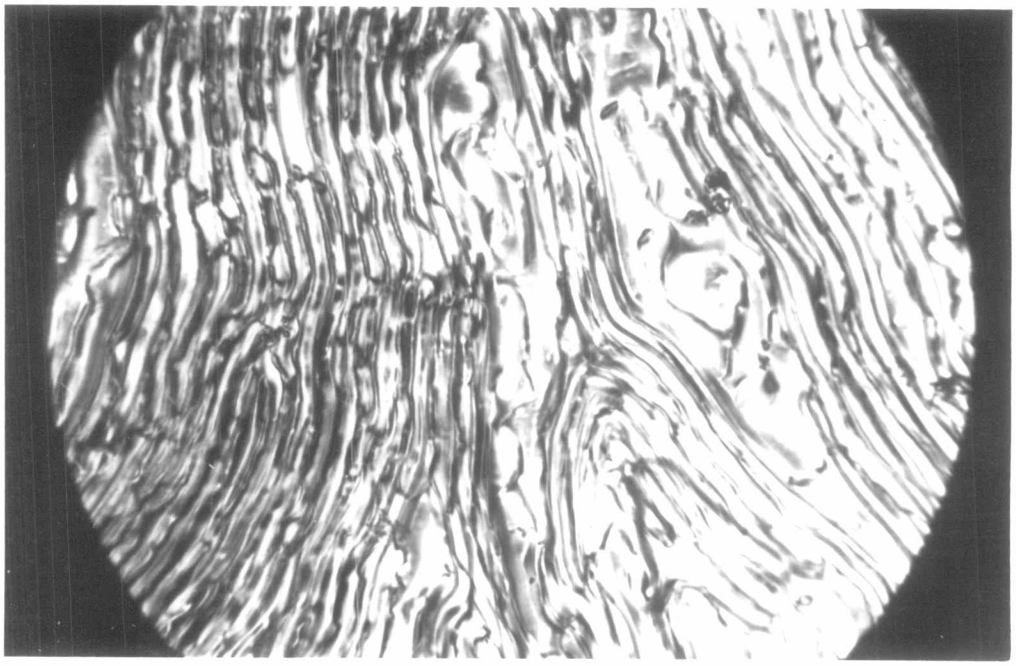

c) T = 132° C (near isotropic transition temperature)

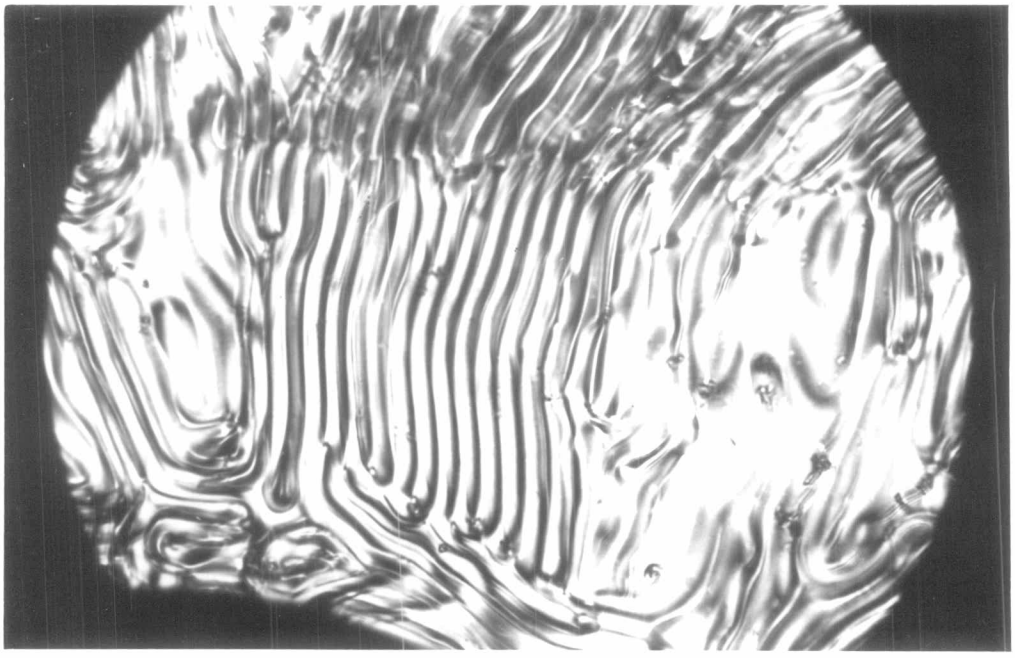

d) T = 132.1° C, different heating cycle

2.3.2 Variation of cholesteric pitch with cholesteric concentration

Heating rate was found to have a noticeable effect on the configulation of the stripes of the cholesteric system. Fast heating rates resulted in small areas of patterns of parallel stripes, whereas slow heating rates yielded larger areas of parallel stripes. Therefore, the slow heating rate 0.2^{o}C/min of the Mettler F5 Temperature Control Unit was used for the rest of the experiment. The resulting stripe patterns of the PAA/CP systems at different cholesteric concentrations and temperatures are shown in Figs. 13 and 14.

The pitch, or how tightly the induced helix is wound, depends sensitively on the concentration of cholesterol ester in the mixture. The systems PAA/CP and MBBA/CP were studied. The results are shown in Table 2 and plotted in Fig. 15.

Table 2 Variation of cholesteric pitch with cholesteric concentration

a) PAA/CP

film thickness = 150 μm, T = 120°C.

c(% of CP)	$\frac{1}{c}$	Pitch (μm)
2.00	0.50	7.00
1.00	1.00	14.36
0.75	1.33	17.54
0.50	2.00	26.32
0.40	2.50	35.09
0.30	3.33	43.86
0.20	5.00	65.79

b) MBBA/CP

film thickness = 50 μm, T = 32°C

c(% of CP)	$\frac{1}{c}$	Pitch (μm)
2.0	0.50	5.26
1.5	0.67	7.36
1.0	1.00	8.77
0.5	2.00	17.89
0.4	2.50	24.56
0.3	3.33	31.92
0.2	5.00	49.12

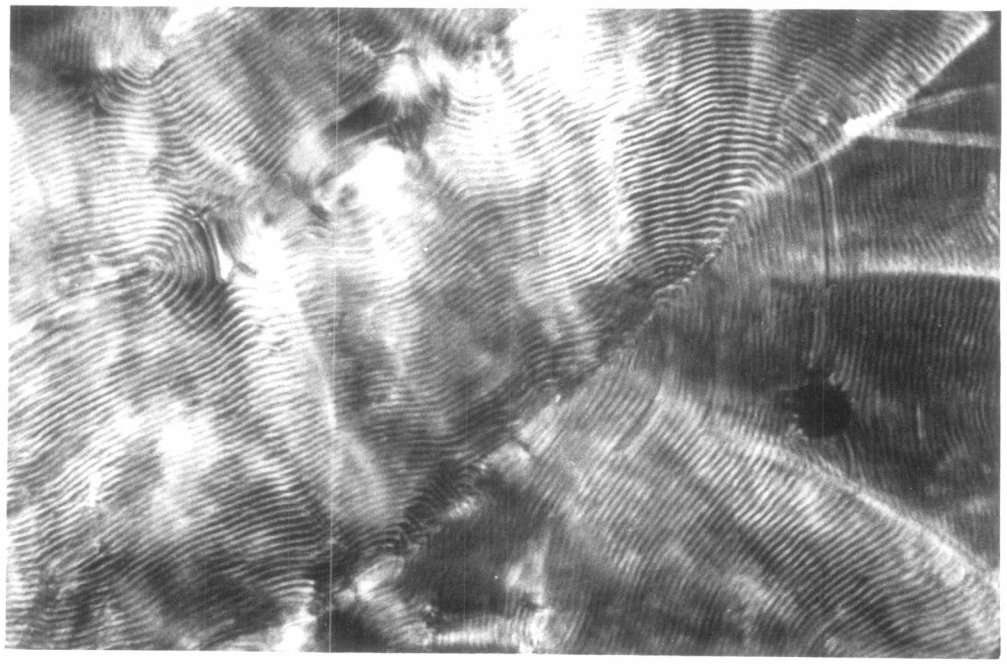

Fig. 13 a) PAA doped with 2 % CP showning the cholesteric pitch $z_o \sim 7$ μm , at temperature $T = 120^oC$

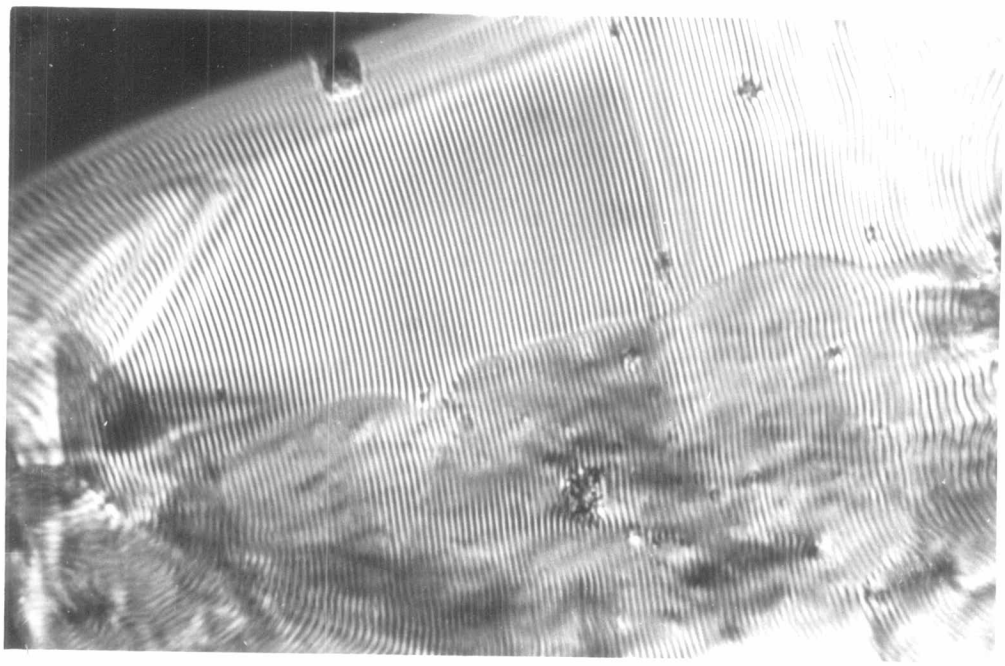

Fig. 13 b) $c = 2\ \%$, $T = 132.6^oC$ and $z_o \sim 7$ μm .

Fig. 13 c) PAA doped with 1 % CP showing cholesteric pitch $z_o \sim 14$ μm, at temperature $T = 120^{o}C$

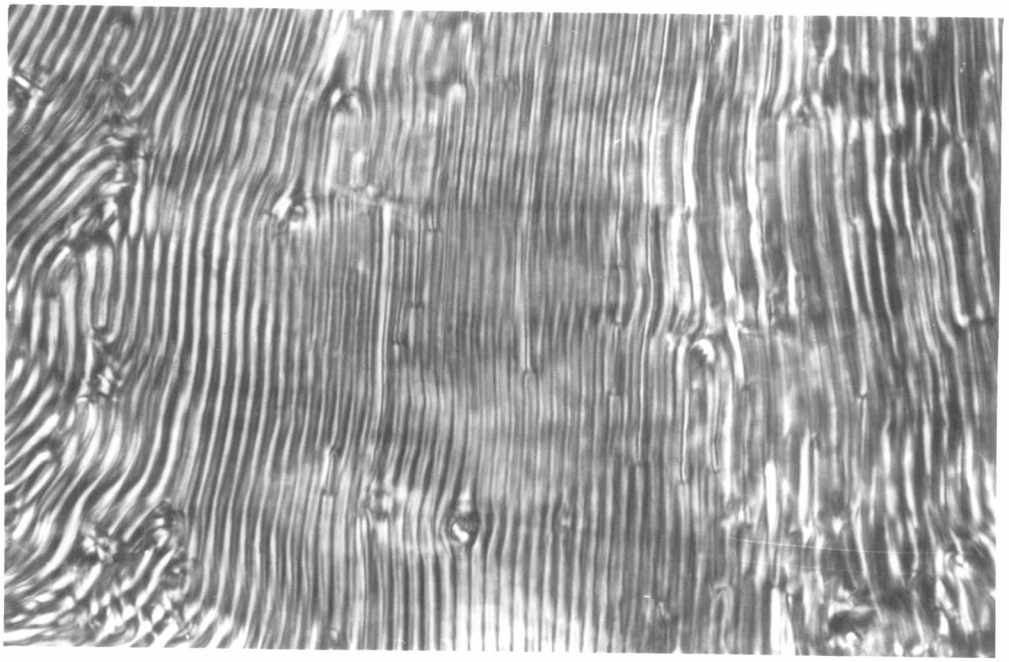

Fig. 13 d) c = 1 %, at $T = 132^{o}C$

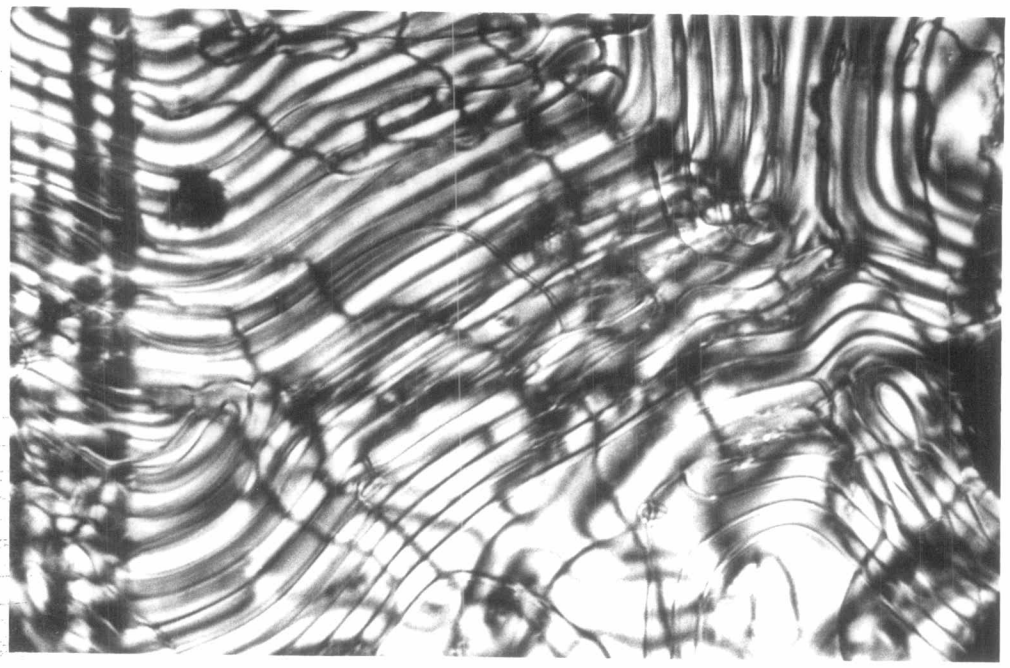

Fig. 13 e) PAA doped with 0.5 % CP showing the cholesteric pitch $z_o \sim$ 26 μm, at temperature T = 120°C

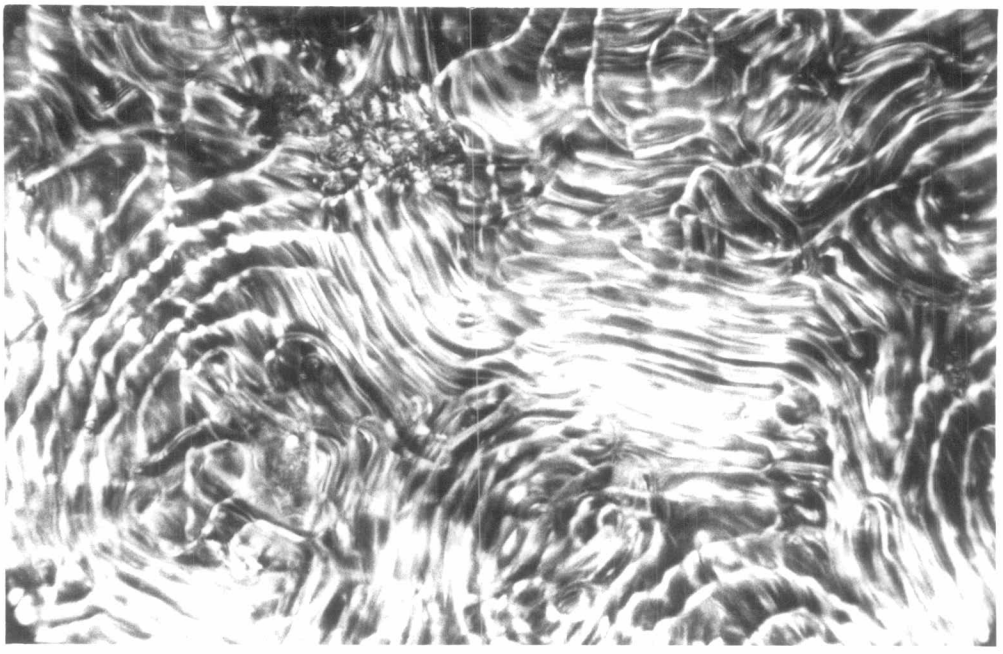

Fig. 13 f) PAA doped with 0.4 % CP showing the cholesteric pitch $z_o \sim$ 35 μm, at temperature T = 120°C

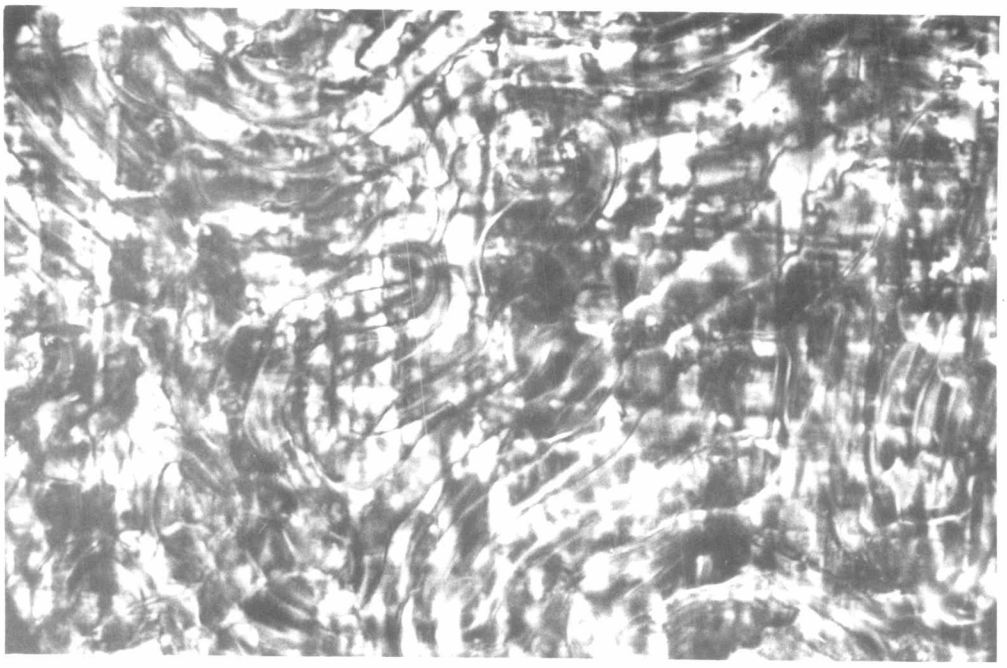

Fig. 13 g) PAA doped with 0.3 % CP showing the cholesteric pitch $z_o \sim 44$ μm, at temperature $T = 120^oC$.

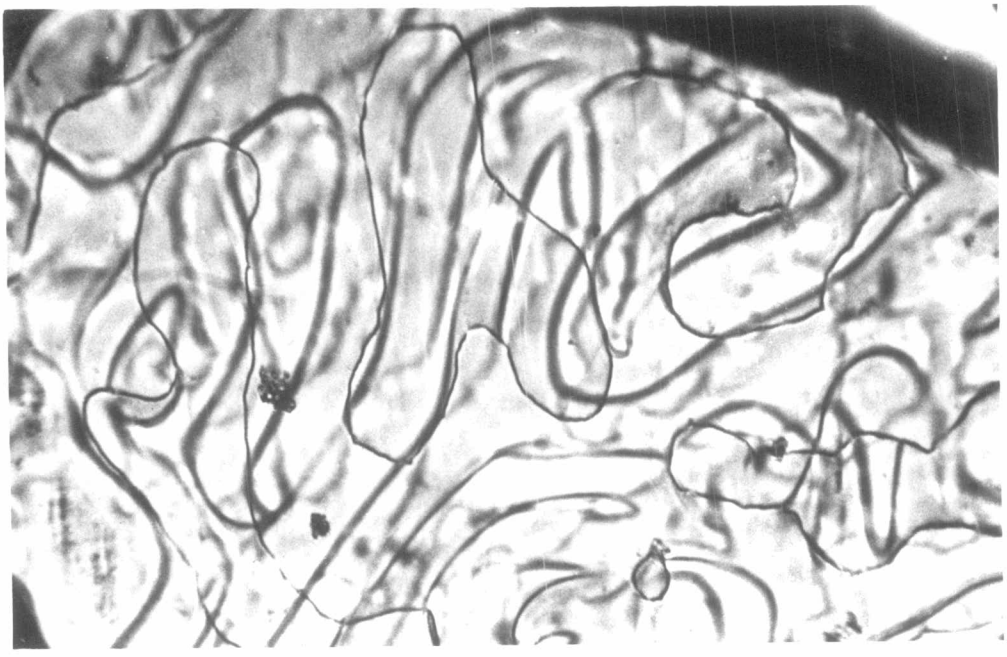

Fig. 13 h) PAA doped with 0.2 % CP showing the cholesteric pitch $z_o \sim 66$ μm, at temperature $T = 120^oC$

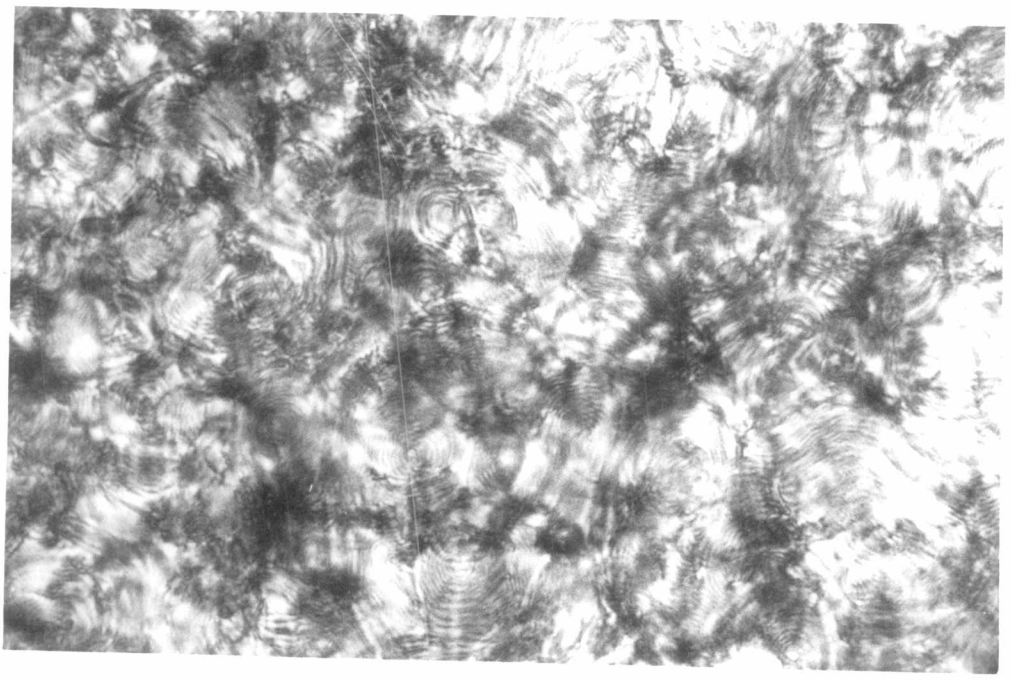

Fig. 14 a) MBBA doped with 2 % CP showing the cholesteric pitch $z_o \sim 5$ µm, at temperature $T = 32^oC$

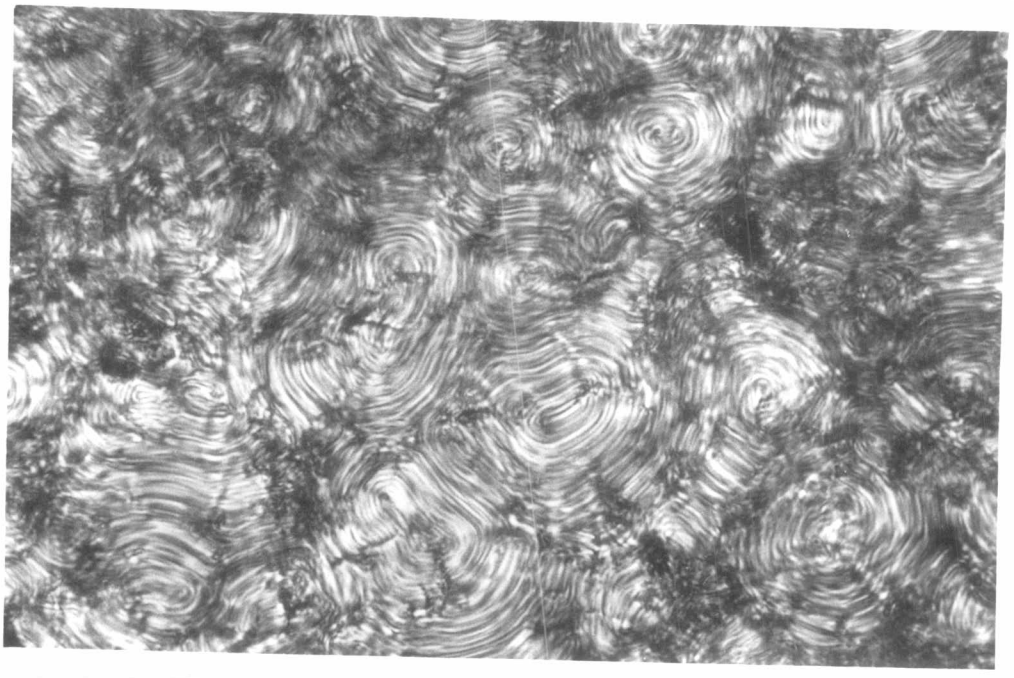

Fig. 14 b) $^c = 1.5$ %, $z_o \sim 7$ µm.

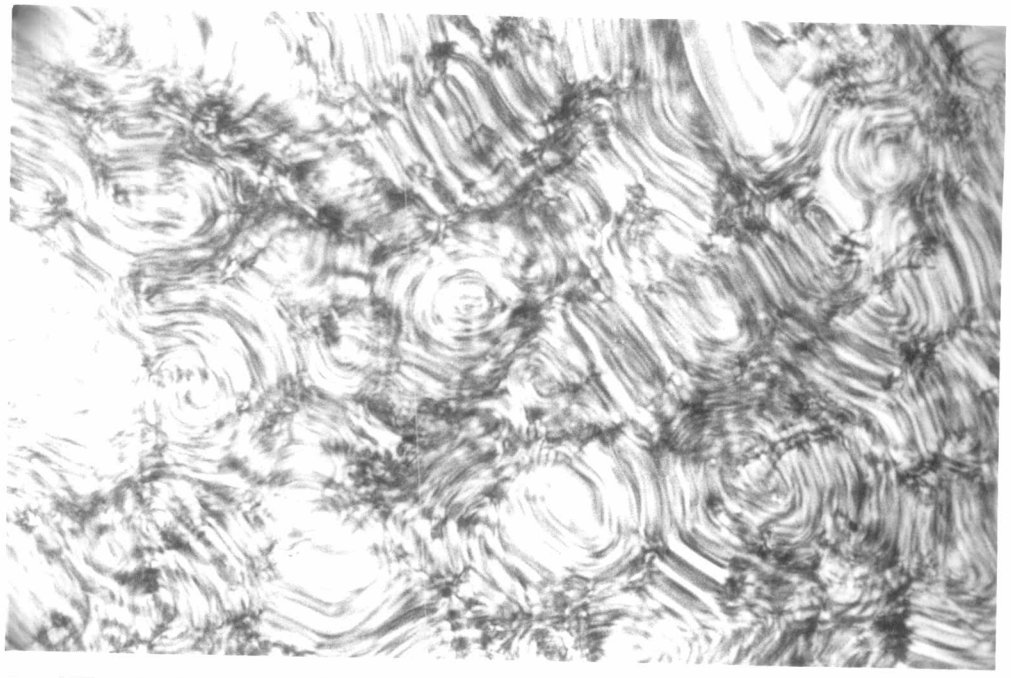

Fig. 14 c) $c = 1\ \%$, $z_o \sim 9\ \mu m$.

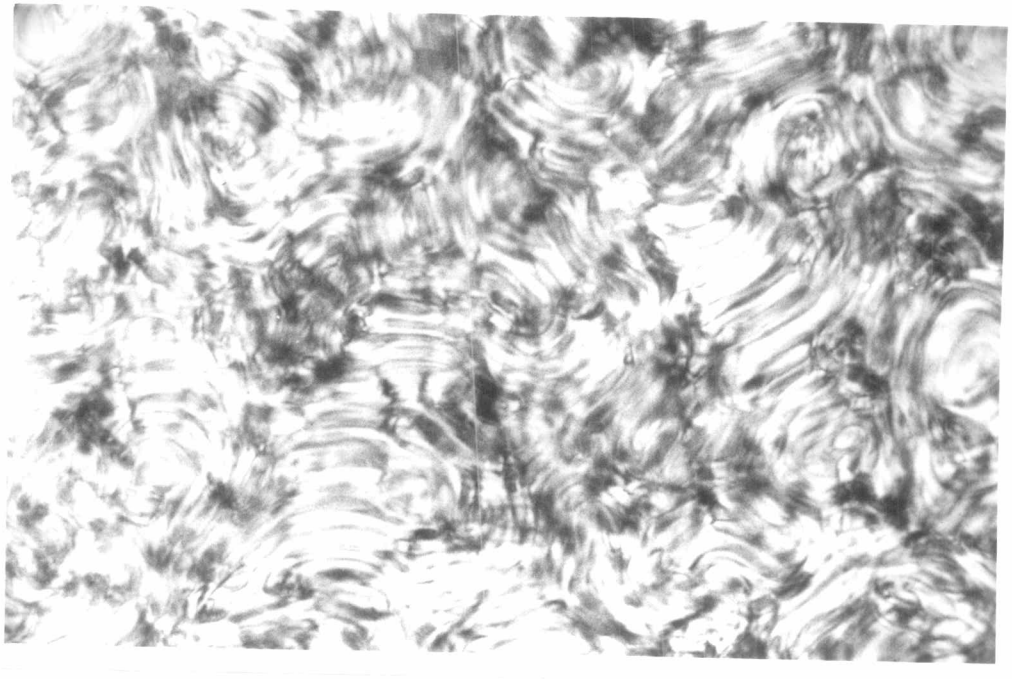

Fig. 14 d) $c = 0.5\ \%$, $z_o \sim 18\ \mu m$.

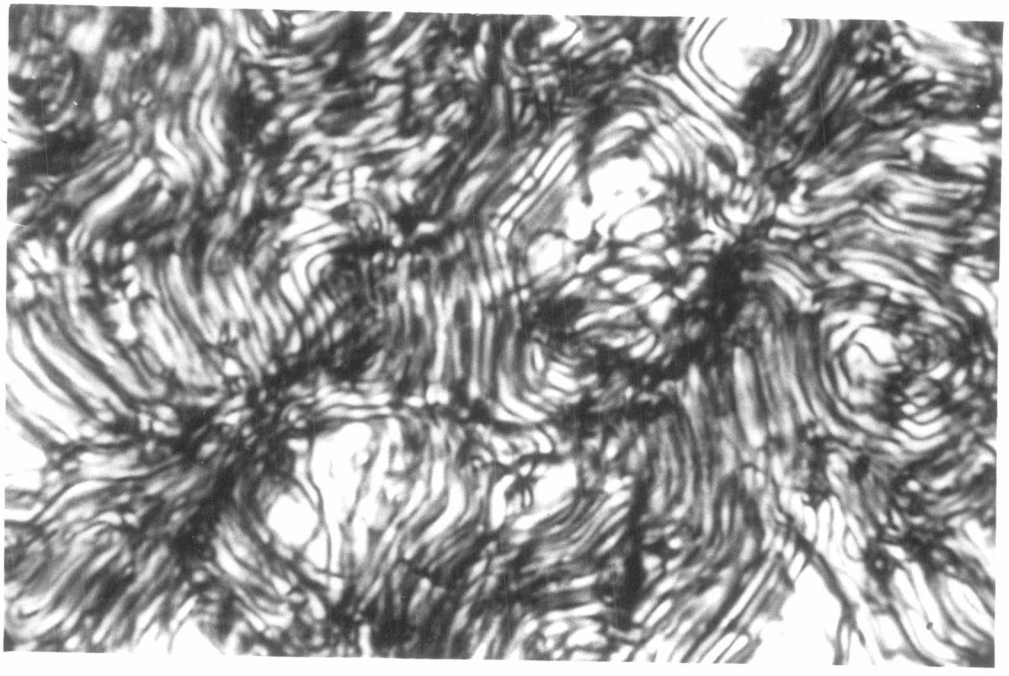

Fig. 14 e) ε = 0.4 %, $z_o \sim 25$ µm.

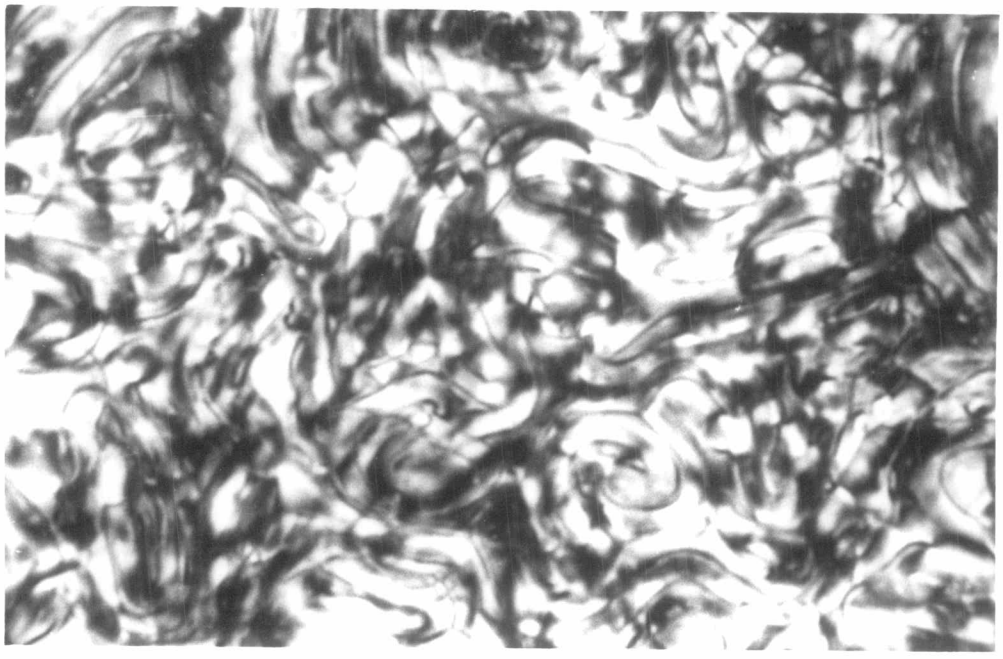

Fig. 14 f) ε = 0.3 %, $z_o \sim 32$ µm.

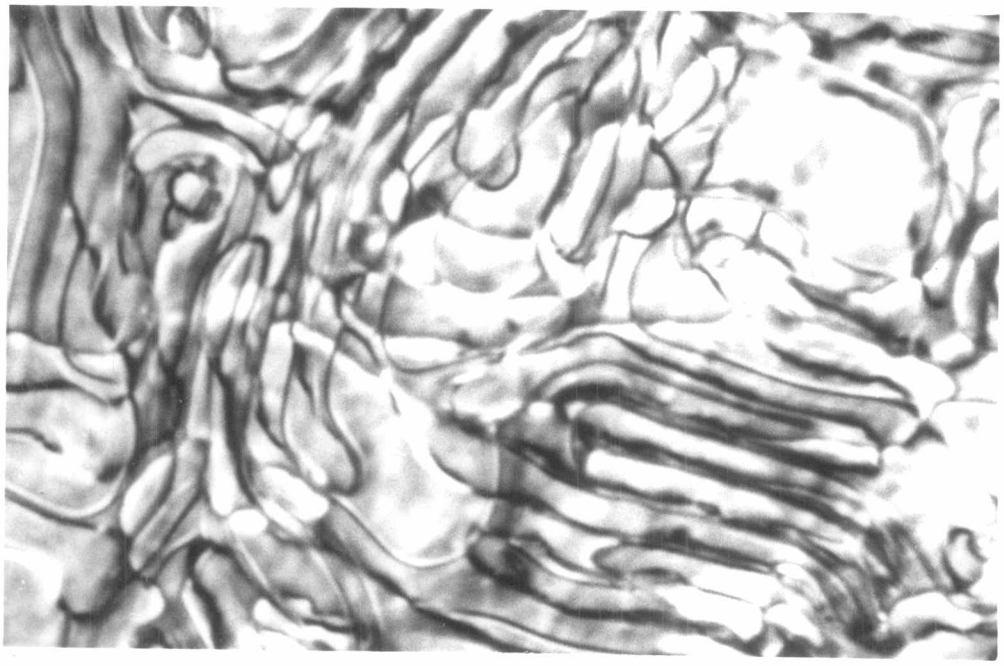

Fig. 14 g) c = 0.3 %, $z_o \sim 49$ µm.

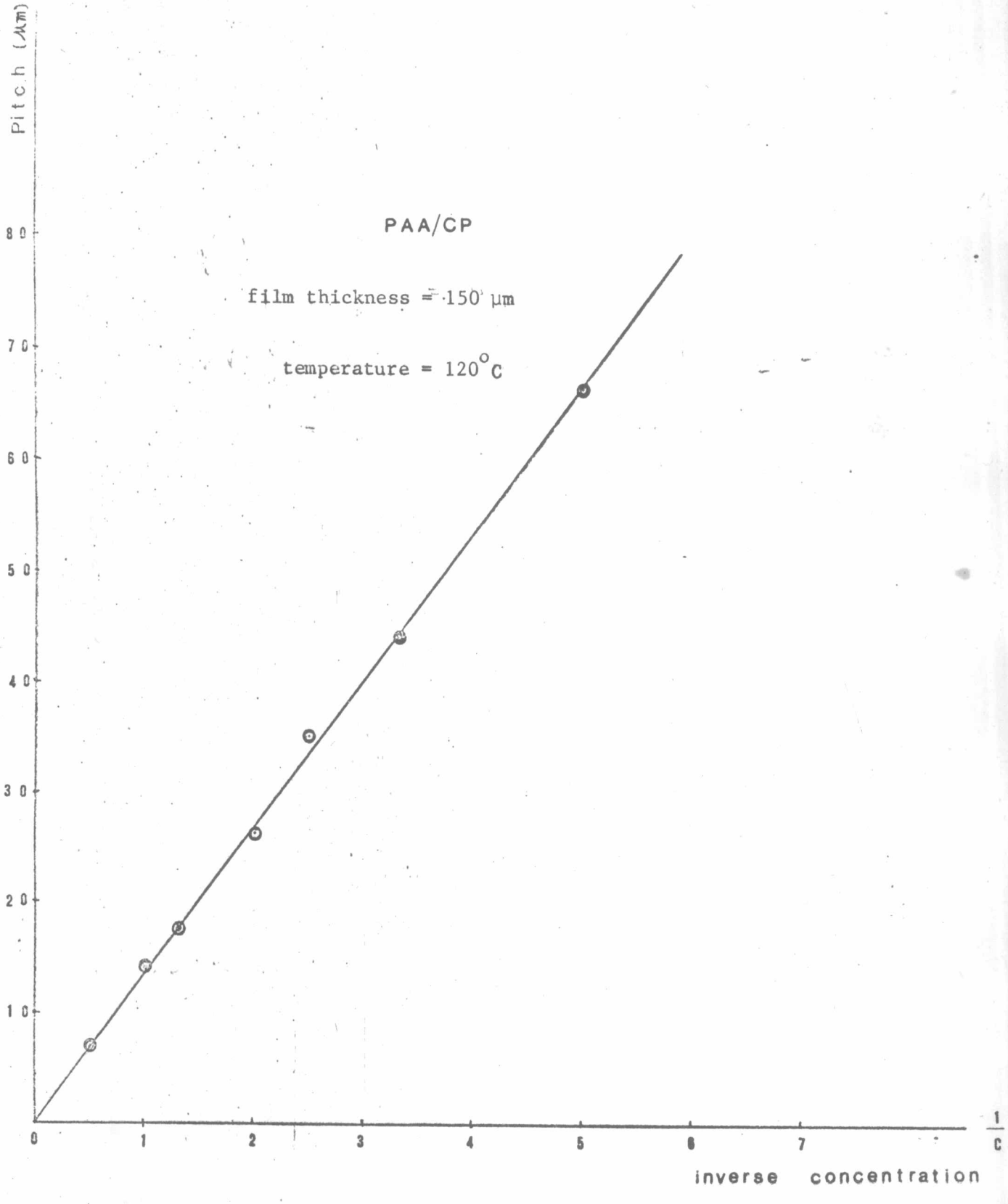

Fig. 15a Pitch vs Inverse Concentration

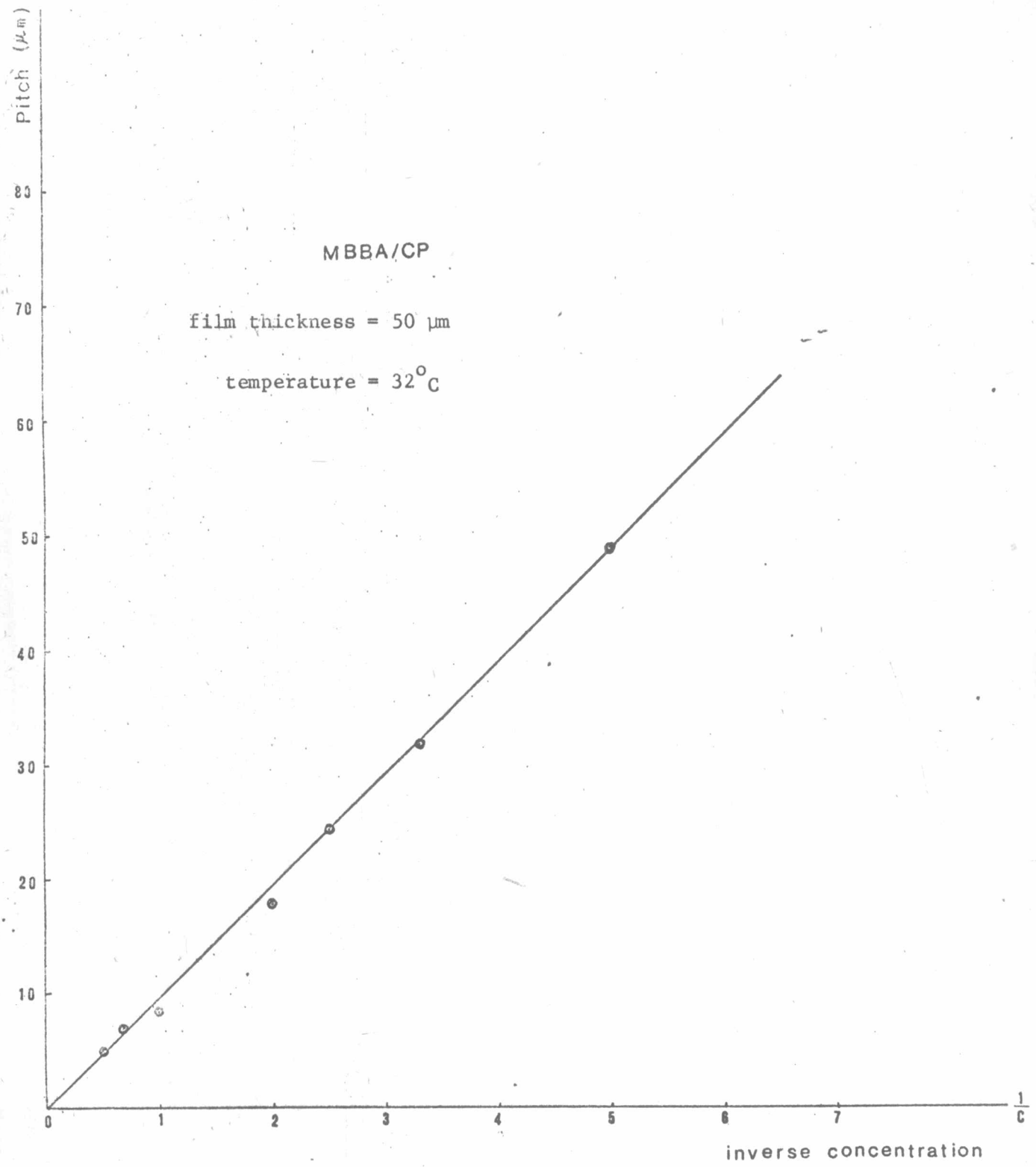

Fig. 15b Pitch vs Inverse Concentration

2.3.3 Variation of cholesteric pitch with magnetic field strength

In this section the dilation of the cholesteric pitch in magnetic field for the system PAA/CP (0.75, 0.5, 0.4, 0.3 and 0.2 %) is reported. The experimental data are shown in Table 3 and Fig. 16. The pitch dilation is shown only for PAA/CP(0.5 %) in the series of photographs in Fig. 17 for film thickness of 150 μm and in Fig. 18 for film thickness of 125 μm.

Table 3 Dilation of cholesteric pitch in magnetic field of PAA/CP at temperature 120°C and film thickness ~ 150 μm

a) c = 0.75 %

Field (kG)	Pitch (μm)
0	17.544
1.0	17.544
2.0	17.544
3.0	17.763
4.0	17.982
5.0	17.982
6.0	18.421
7.0	18.860
7.5	20.176
8.0	21.053
8.4	24.123
8.5	27.193
8.534	unobservable

b) $c = 0.5\ \%$

Field (kG)	Pitch (μm)
0	26.316
0.55	26.316
1.00	26.316
1.50	26.316
2.00	26.316
3.00	26.754
4.00	28.070
4.50	28.947
5.00	30.263
5.35	32.895
5.50	35.086
5.55	36.842
5.60	39.474
5.63	42.105
5.656	unobservable

c) ϵ = 0.4 %

Field (kG)	Pitch (μm)
0	35.087
1.0	35.087
1.5	35.087
2.0	35.087
2.5	35.526
3.0	35.965
3.4	36.842
3.7	37.719
3.9	38.596
4.2	40.790
4.4	42.982
4.6	46.052
4.7	50.440
4.75	57.018
4.798	unobservable

d) $c = 0.3\ \%$

Field (kG)	Pitch (μm)
0	43.860
1.0	43.860
1.4	43.860
1.8	44.299
2.2	45.176
2.6	46.053
2.8	47.807
3.0	49.123
3.2	52.193
3.3	54.386
3.45	61.404
3.49	67.106
3.494	unobservable

e) $c = 0.2\ \%$

Field (kG)	Pitch (μm).
0	65.790
1.0	65.790
1.6	68.422
1.8	69.737
2.0	72.369
2.2	77.303
2.3	81.580
2.35	82.895
2.40	90.132
2.43	100.878
2.442	unobservable

Fig.16 Dilation of cholesteric pitch in magnetic field.

Solid curve is from de Gennes[12]

a) PAA/CP(0.75%), film thickness d = 150 μm,

T ≒ 120°C, z_0 = 17.54 μm, H_c = 8.534 kG

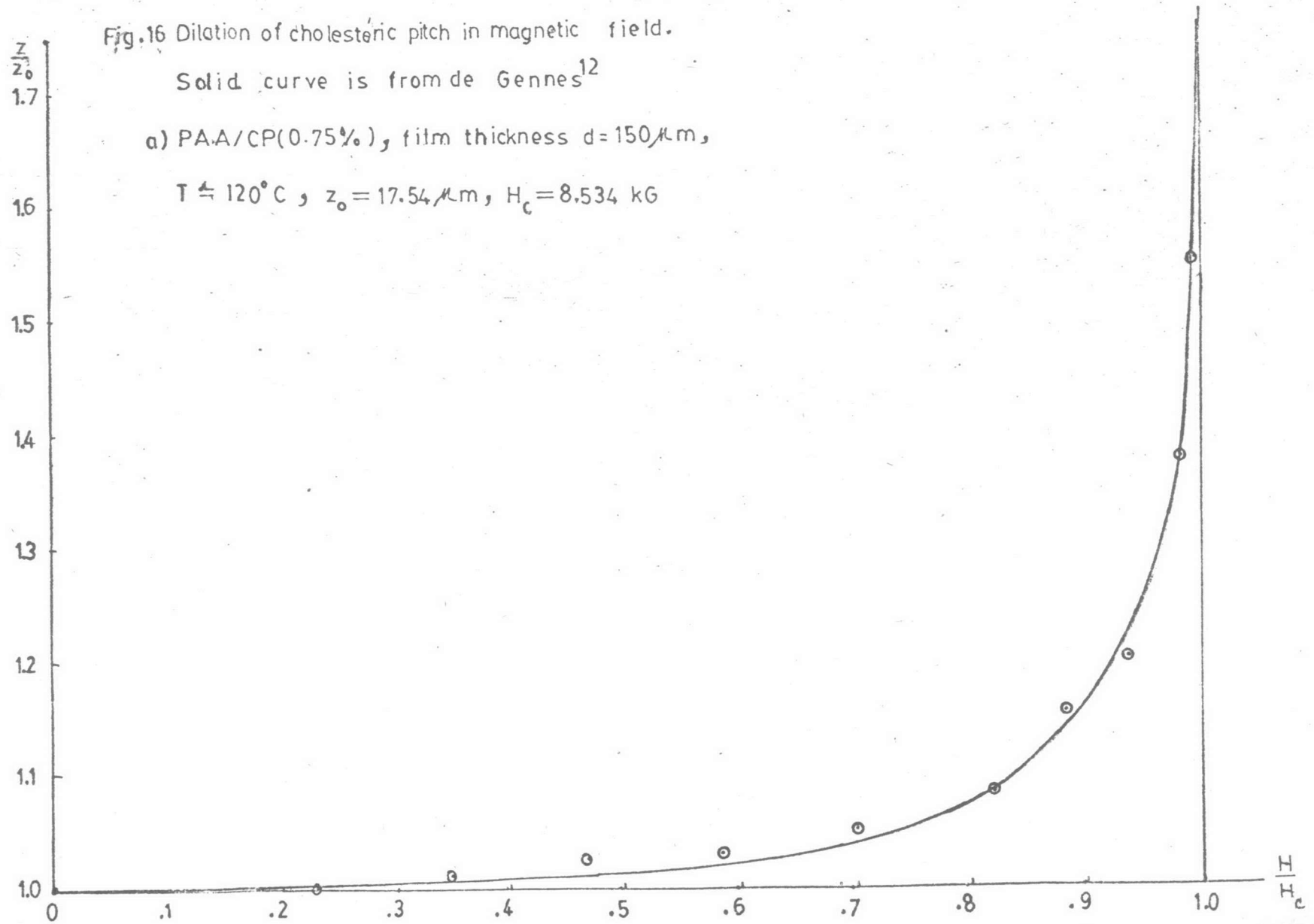

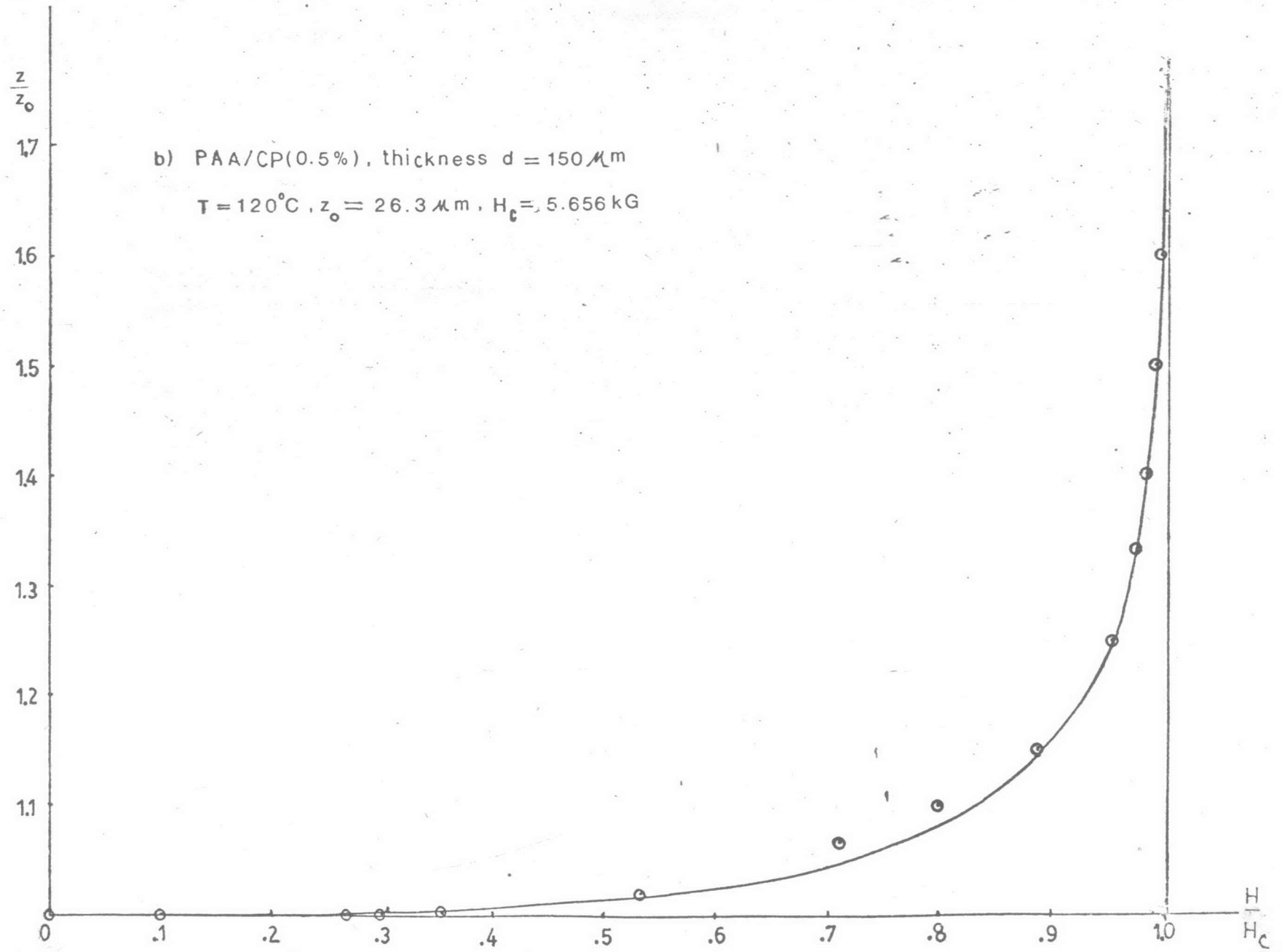
b) PAA/CP(0.5%), thickness d = 150 μm
T = 120°C, z₀ = 26.3 μm, H_c = 5.656 kG
z/z₀
1.7
1.6
1.5
1.4
1.3
1.2
1.1
0
.1
.2
.3
.4
.5
.6
.7
.8
.9
1.0
H/H_c

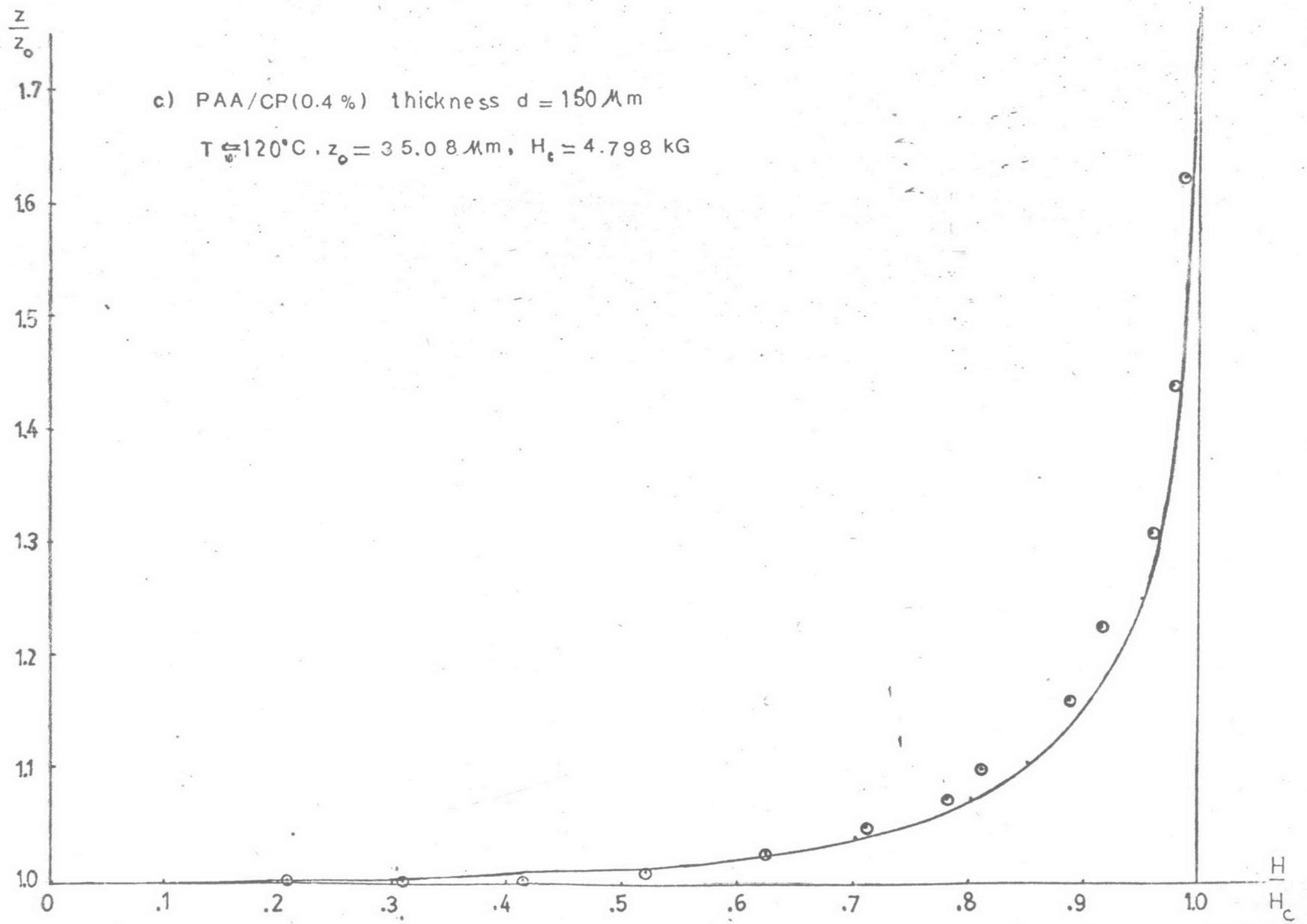
c) PAA/CP(0.4 %) thickness d = 150 Mm
T ≒ 120°C , z₀ = 35.08 Mm , H_c = 4.798 kG
z/z₀
1.7
1.6
1.5
1.4
1.3
1.2
1.1
1.0
0
.1
.2
.3
.4
.5
.6
.7
.8
.9
1.0
H/H_c

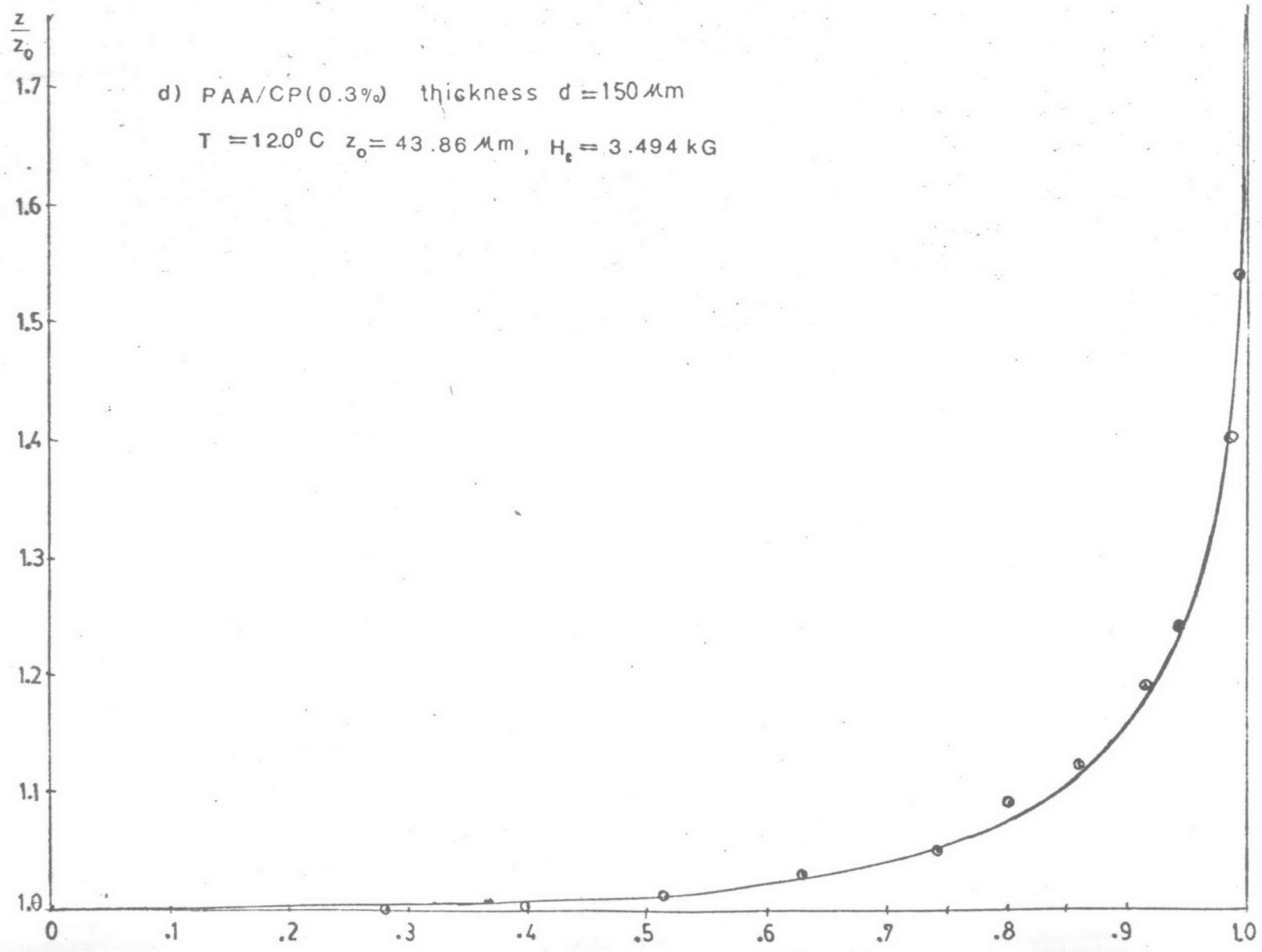
z/z0
d) PAA/CP(0.3%) thickness d = 150 μm
T = 12.0° C z0 = 43.86 μm , Hc = 3.494 kG
1.7
1.6
1.5
1.4
1.3
1.2
1.1
1.0
0
.1
.2
.3
.4
.5
.6
.7
.8
.9
1.0
H/Hc

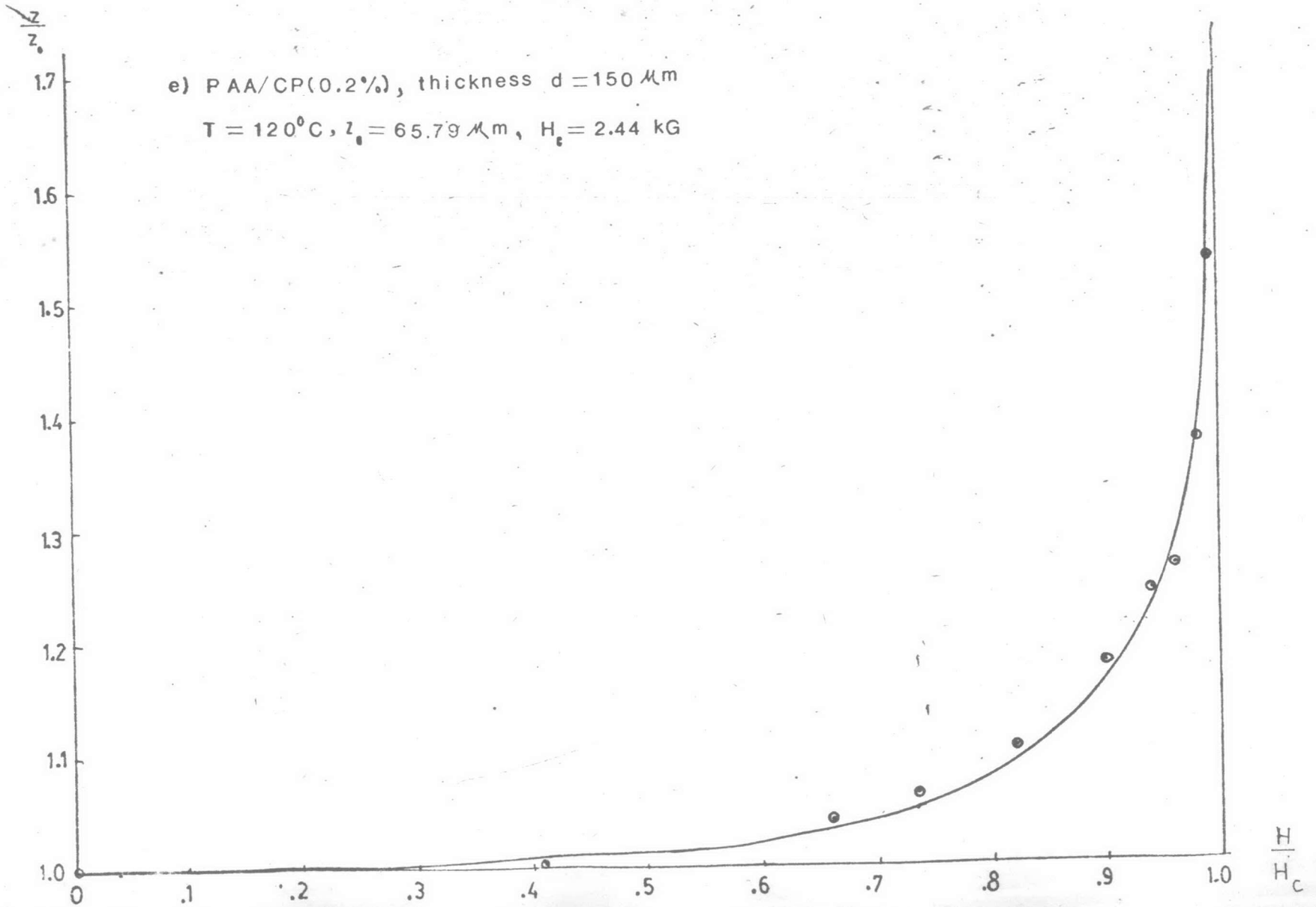
z/z₀
e) PAA/CP(0.2%), thickness d = 150 μm
T = 120°C, z₀ = 65.79 μm, H_c = 2.44 kG
1.7
1.6
1.5
1.4
1.3
1.2
1.1
1.0
0
.1
.2
.3
.4
.5
.6
.7
.8
.9
1.0
H/H_c

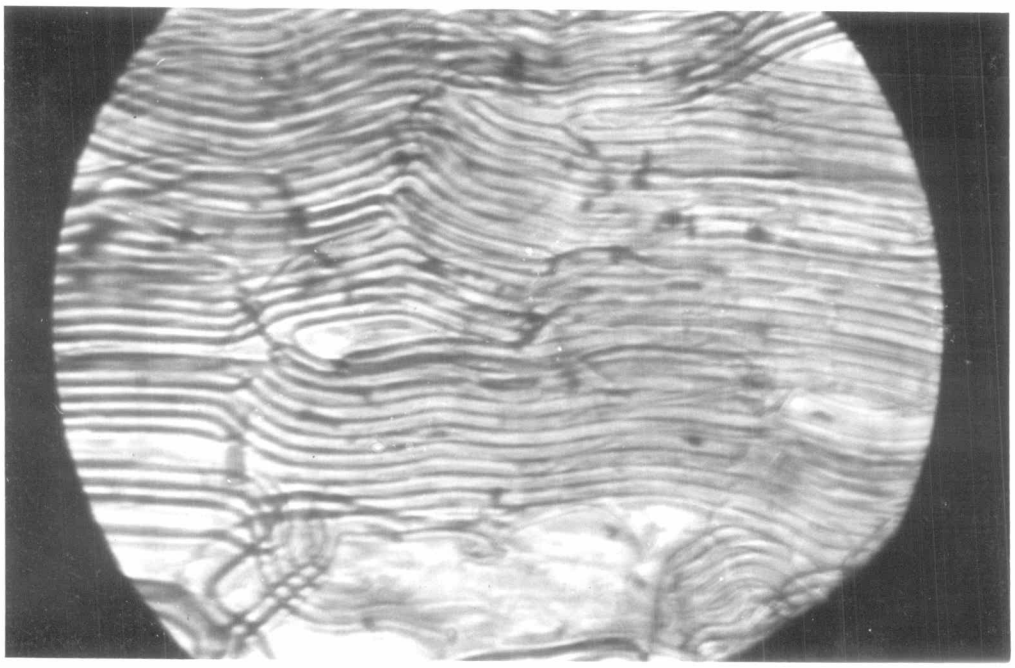

Fig. 17 Dilation of cholesteric pitch in magnetic field in PAA/CP (0.5 %). Sample thickness = 150 μm, T = 120°C. Zero field pitch (z_o) = 26 μm

a). H = 0 kG

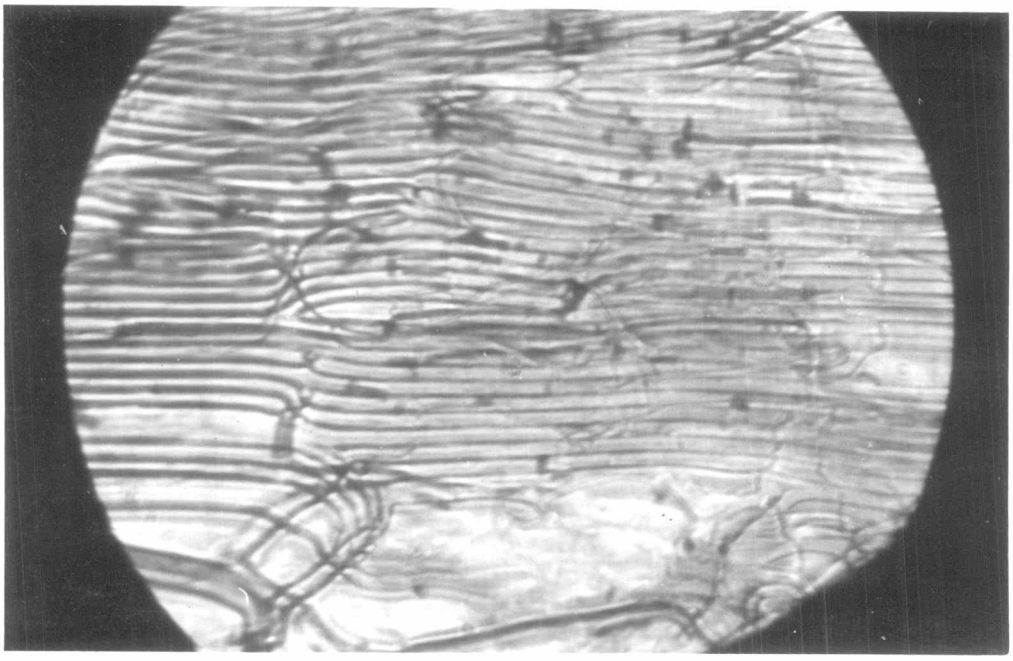

b). H = 2 kG

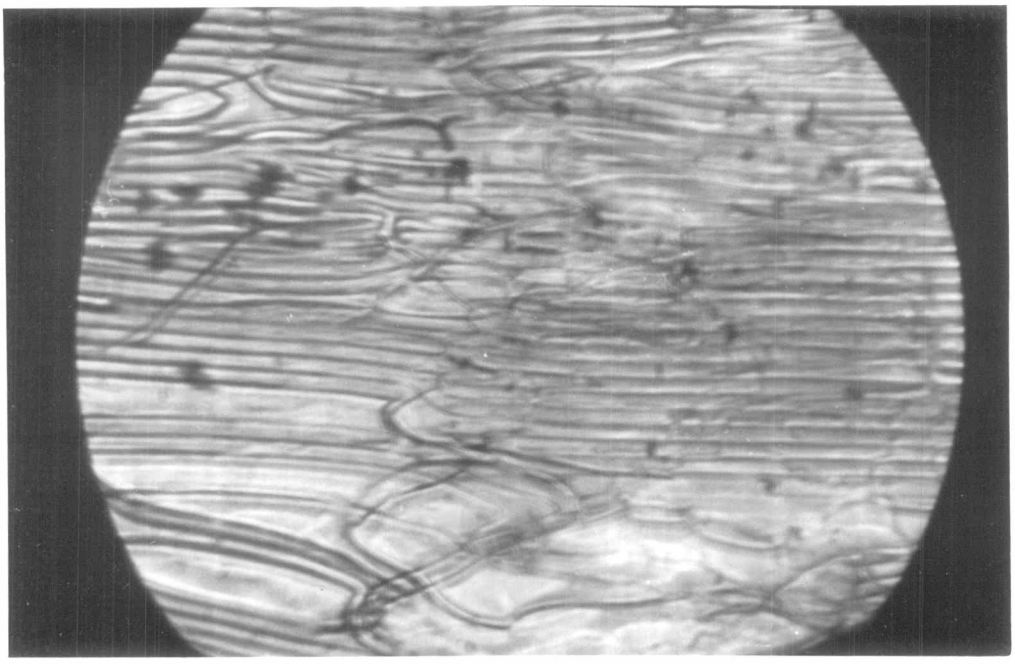

c) H = 4 kG

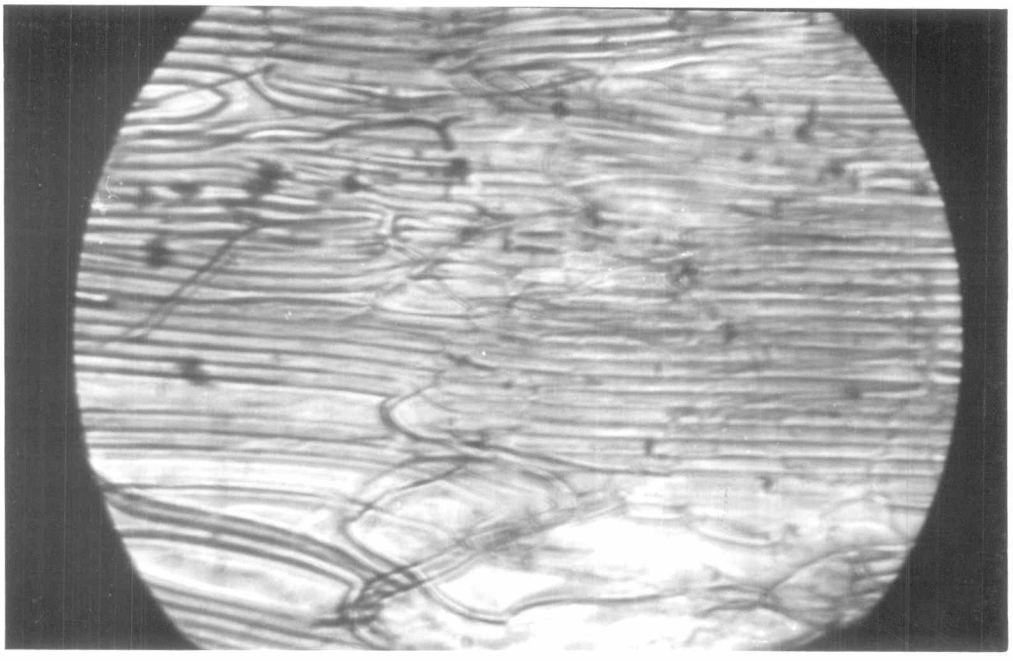

d) H = 4.4 kG

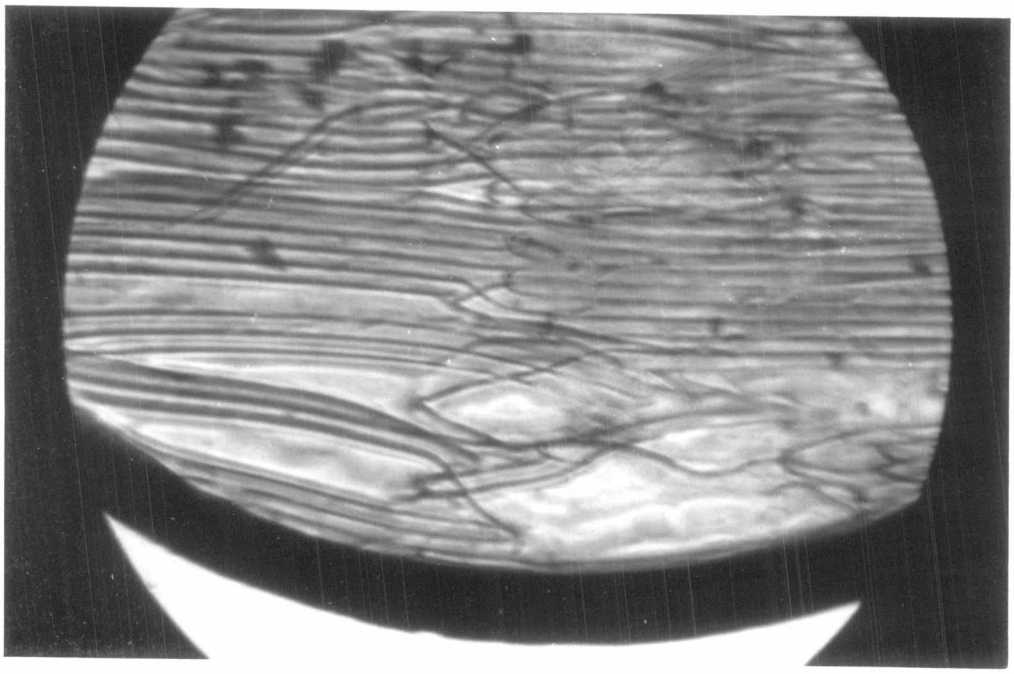

e) H = 4.8 kG

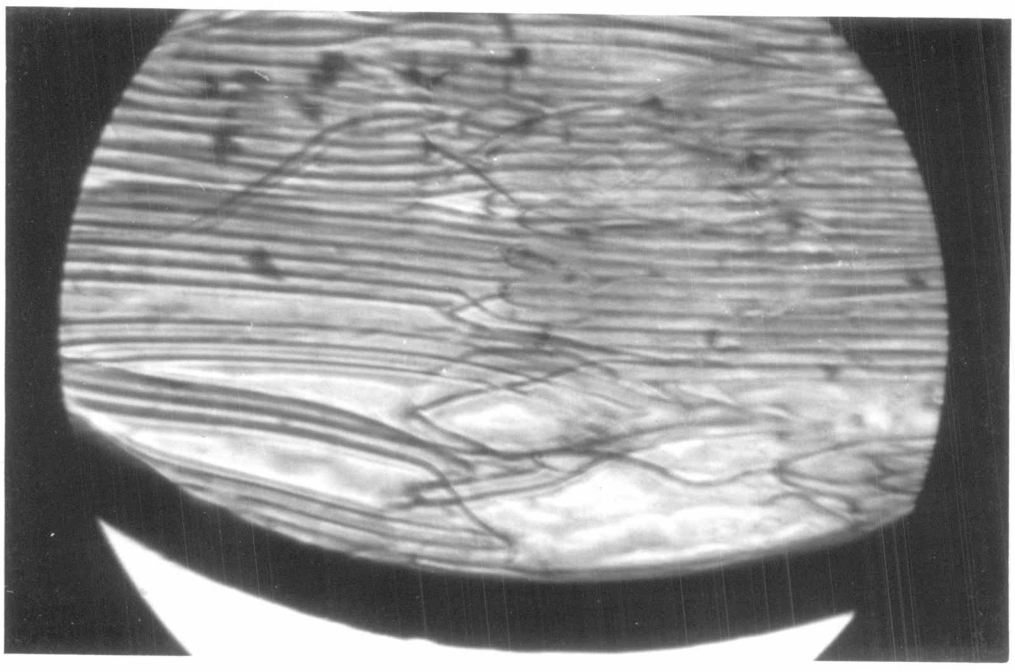

f) H = 4.9 kG

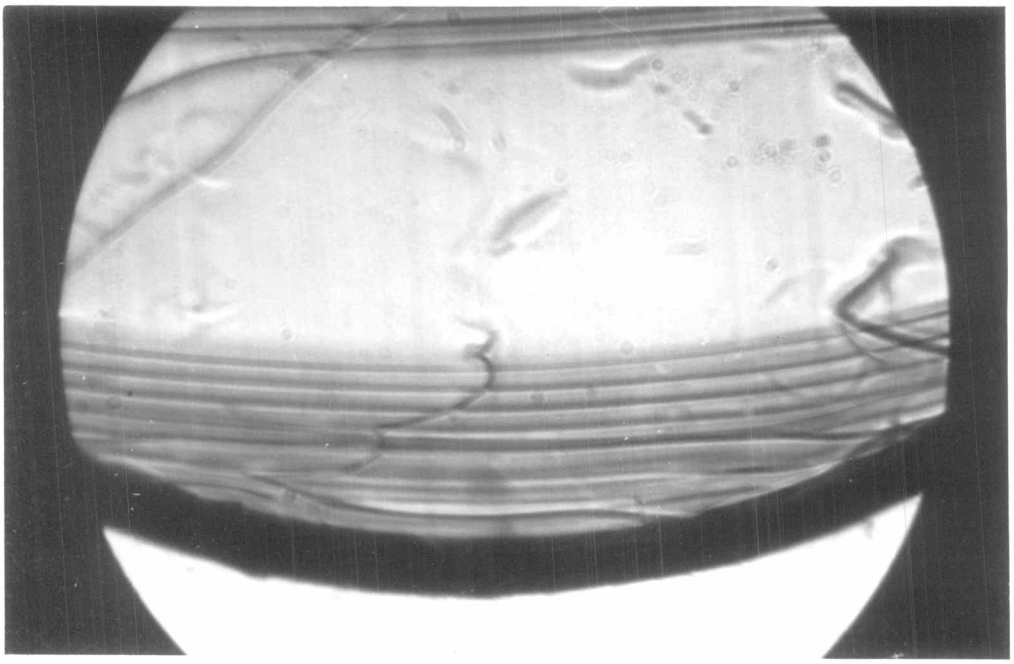

g) H = 5.5 kG

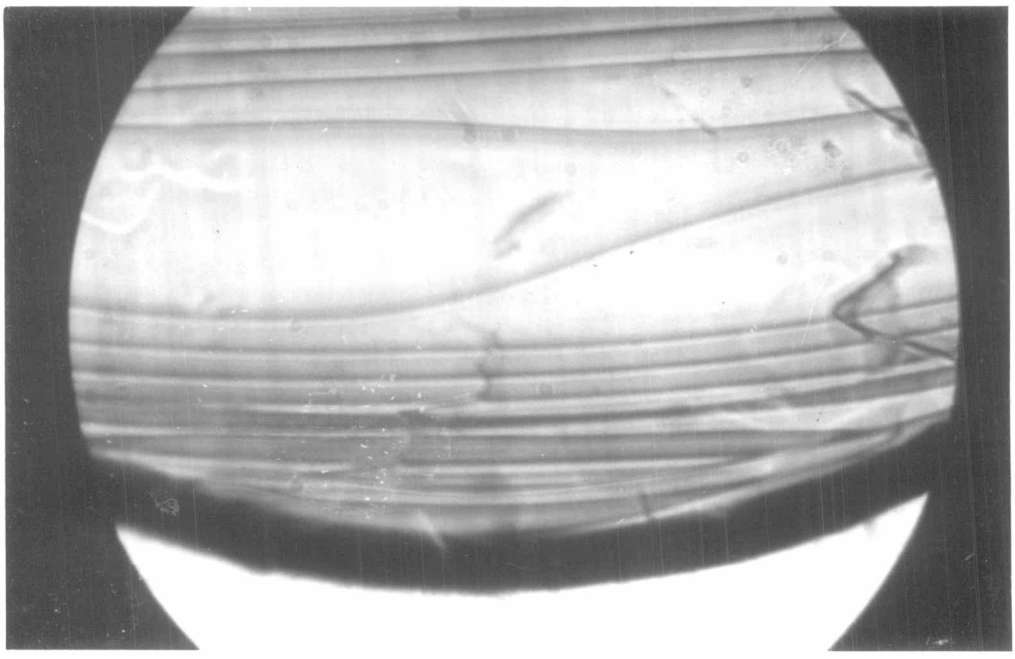

h) H = 5.6 kG

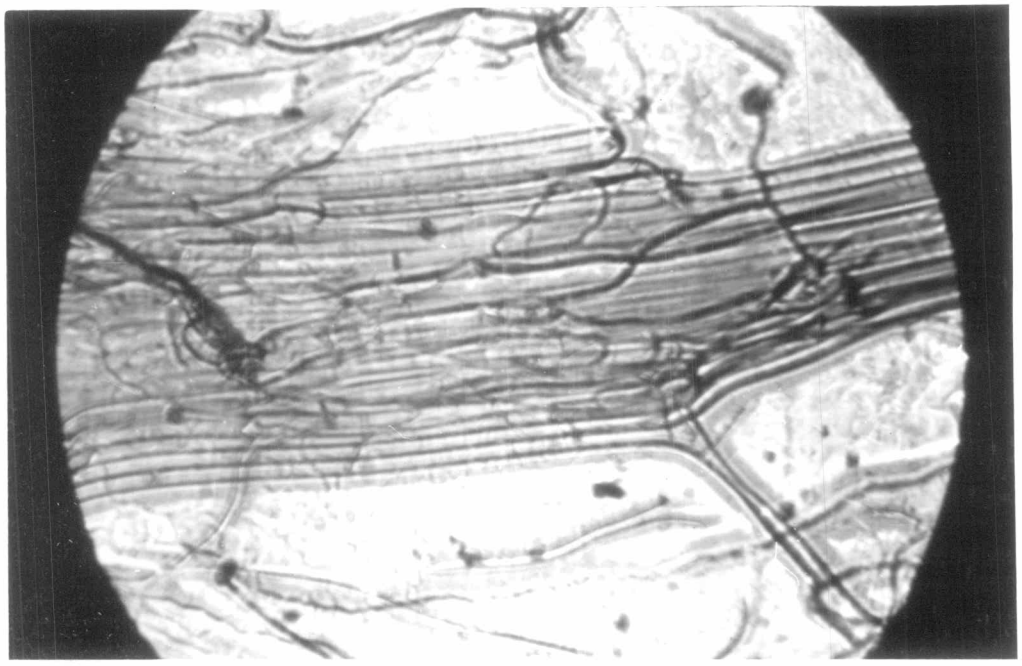

Fig. 18 a) Dilation of cholesteric pitch in magnetic field in PAA/CP (0.5 %), sample thichness = 125 μm , T = 120°C, H = 3.0 kG, pitch ~ 27 μm

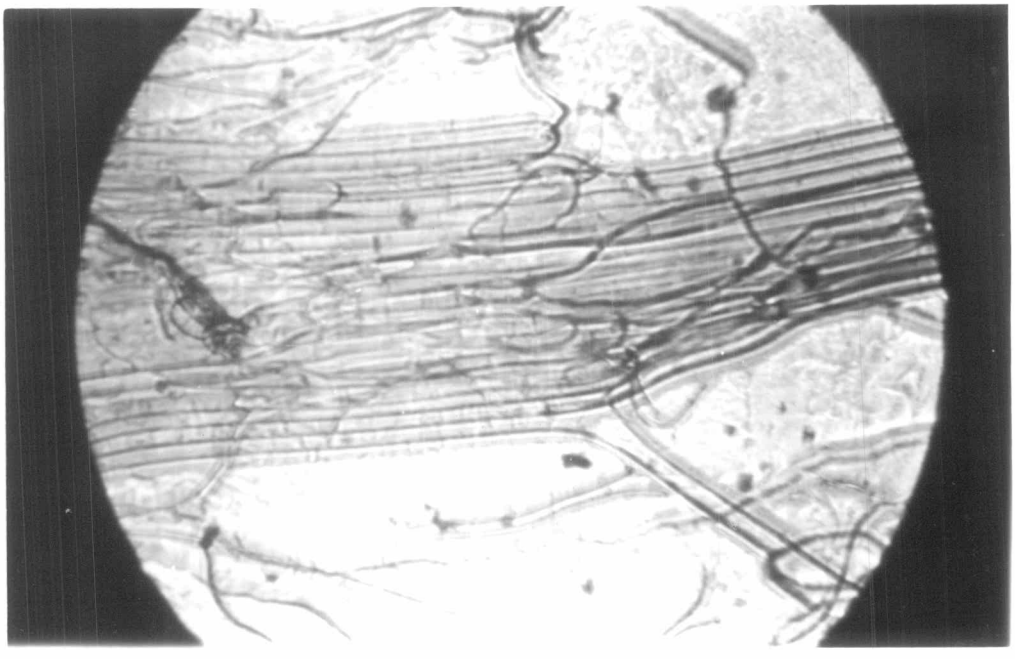

b) The same sample in magnetic field H = 4 kG. Pitch is about 28 μm

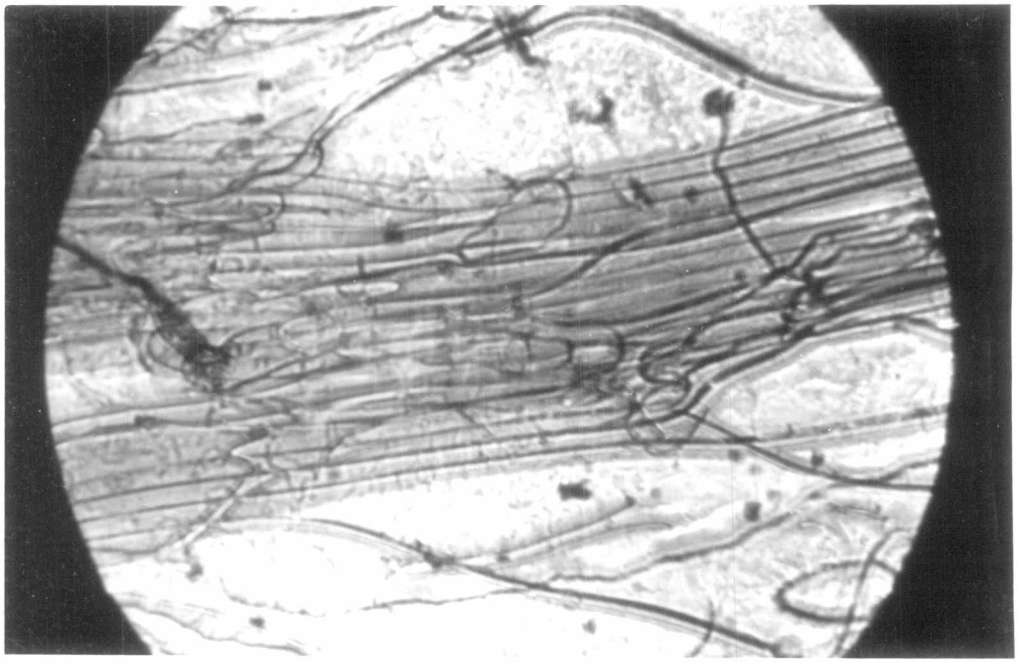

c) The same sample in magnetic field H = 5 kG. Pitch is about 31 μm

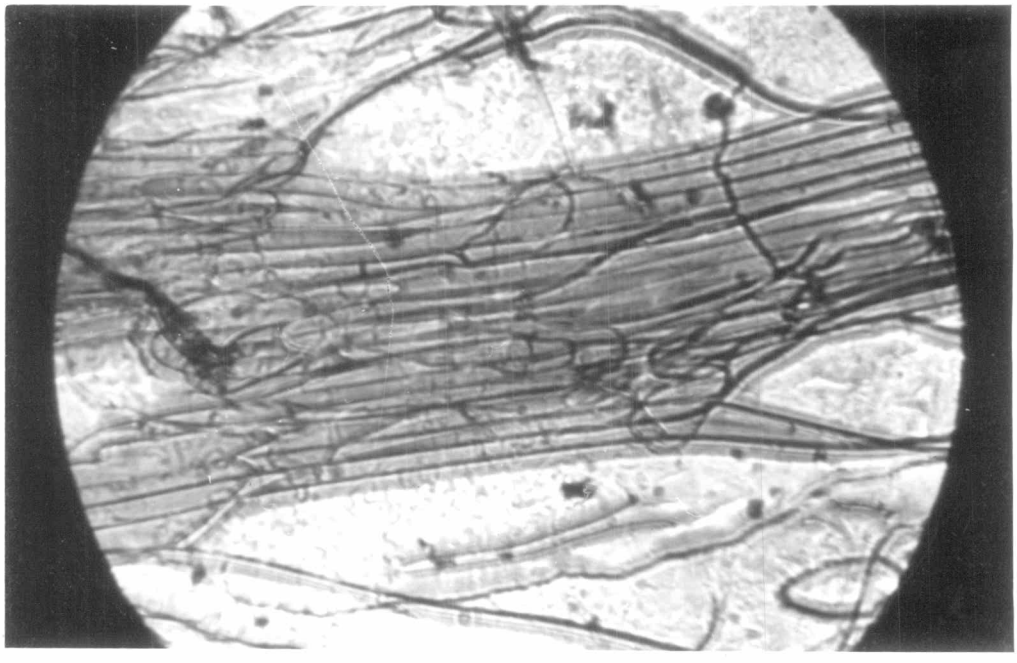

d) The same sample in magnetic field H = 5.4 kG. Pitch is about 34 μm

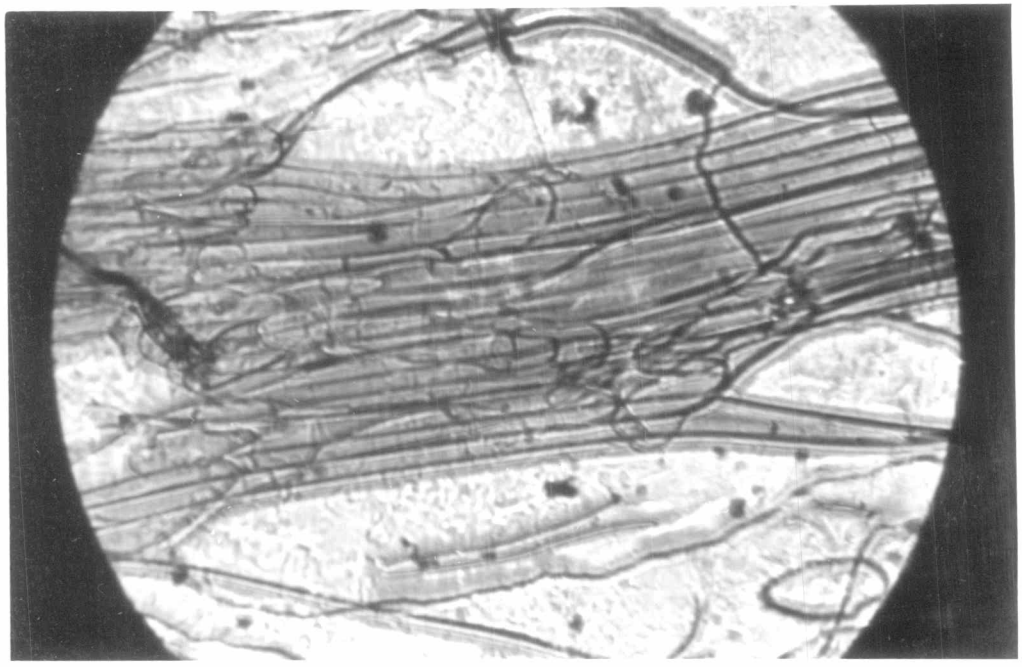

e) The same sample in magnetic field H = 5.5 kG. Pitch is about 37 μm

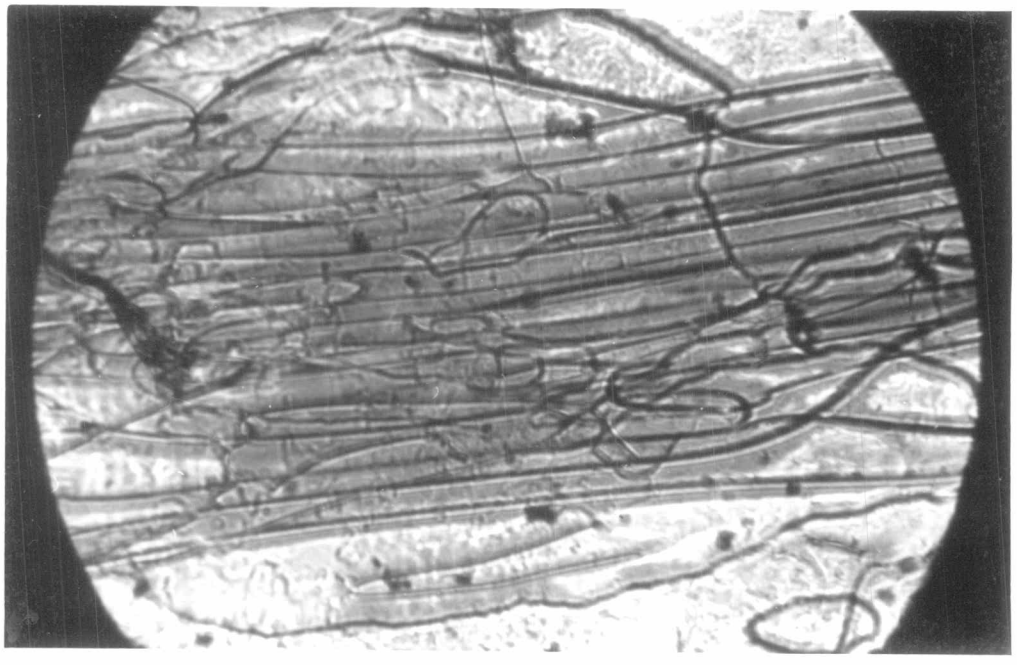

f) The same sample in magnetic field H = 5.6 kG. Pitch is about 39 μm

2.3.4 Critical field dependence on cholesteric concentration

It was mentioned in section 2.3.3 that the value of the critical field depends on the cholesteric concentration in the mixture. The critical field values of mixtures with various concentrations of CP (0.2, 0.3, 0.4, 0.5, 0.75 %) at different temperatures are shown in Table 4. The sample thickness d was 150 m. The critical field values are plotted against concentration in Fig. 19.

Table 4 Dependence of critical field values on the concentration of CP in PAA

	c=0.2%	c=0.3%	c=0.4%	c=0.5%	c=0.75%
T(^{o}C)	H_c(kG)	H_c(kG)	H_c(kG)	H_c(kG)	H_c(kG)
90	2.929	4.120	5.100	6.161	-
100	2.838	4.019	5.050	6.010	10.151
110	2.727	3.898	4.979	5.832	9.292
115	2.626	3.838	4.949	5.757	8.989
117.6	-	-	-	-	8.737
117.7	-	-	-	5.750	-
118	2.565	3.676	4.848	-	-
120	2.442	3.494	4.798	5.656	8.534
125	2.626	3.151	4.360	5.302	7.676
130	2.100	2.908	3.939	4.740	6.868
132.4	-	2.660	3.630	-	-
132.5	1.979	-	-	4.363	6.514

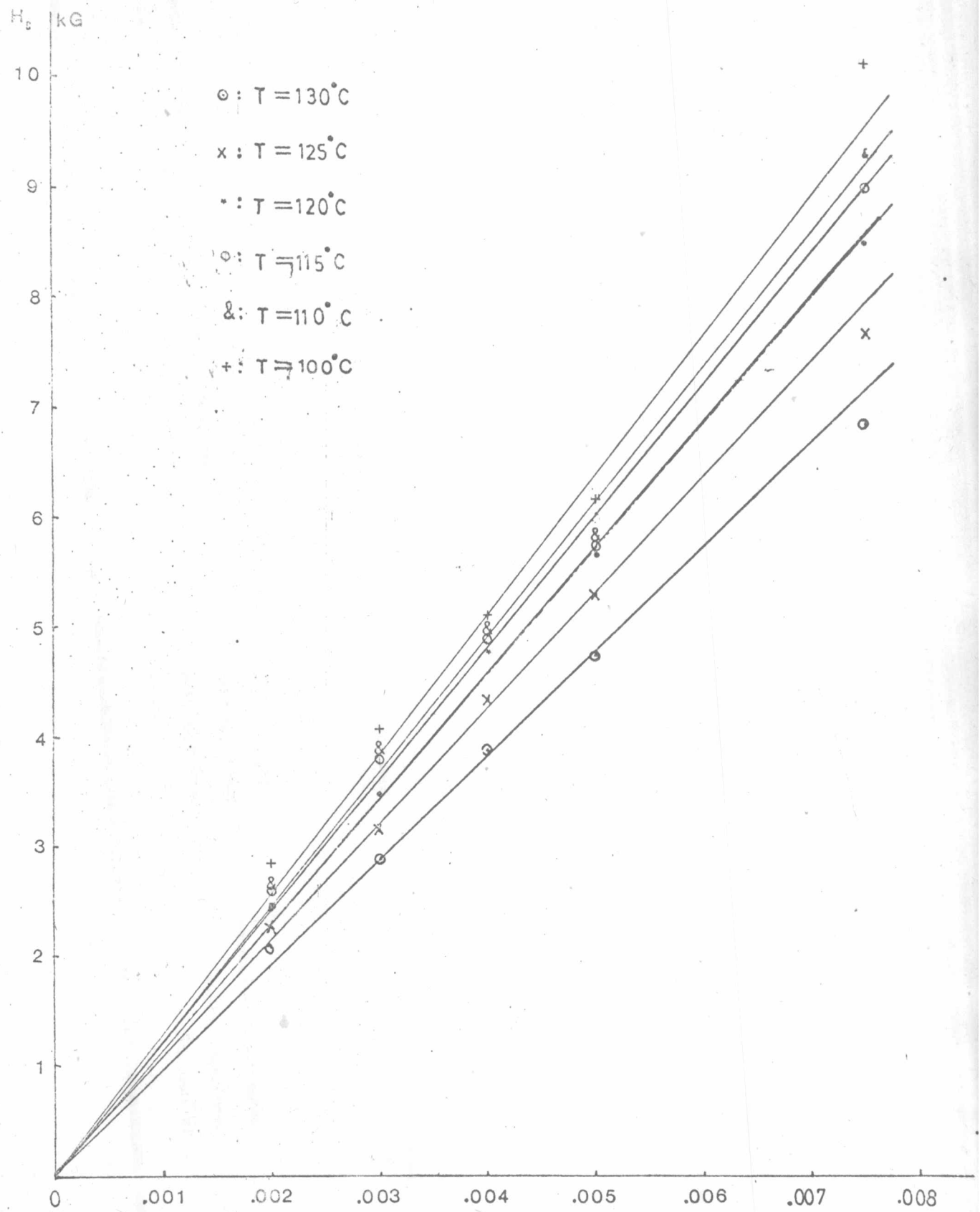

Fig.19 Dependence of critical field upon the concentration of the cholesteric in RAA/CP

2.3.5 Critical field dependence on sample film thickness

The dependence of the critical field strength on sample thickness was studied in the PAA/CP system with CP concentration of 0.5 %. The results are shown in Table 5. The critical field values are Plotted against sample film thickness in Fig. 20.

Table 5 Critical field dependence on sample film thickness

Thickness (μm)	H_c (kG)
30	5.670
50	5.670
75	5.670
100	5.665
125	5.656
150	5.656
200	5.655
250	5.655
300	5.655

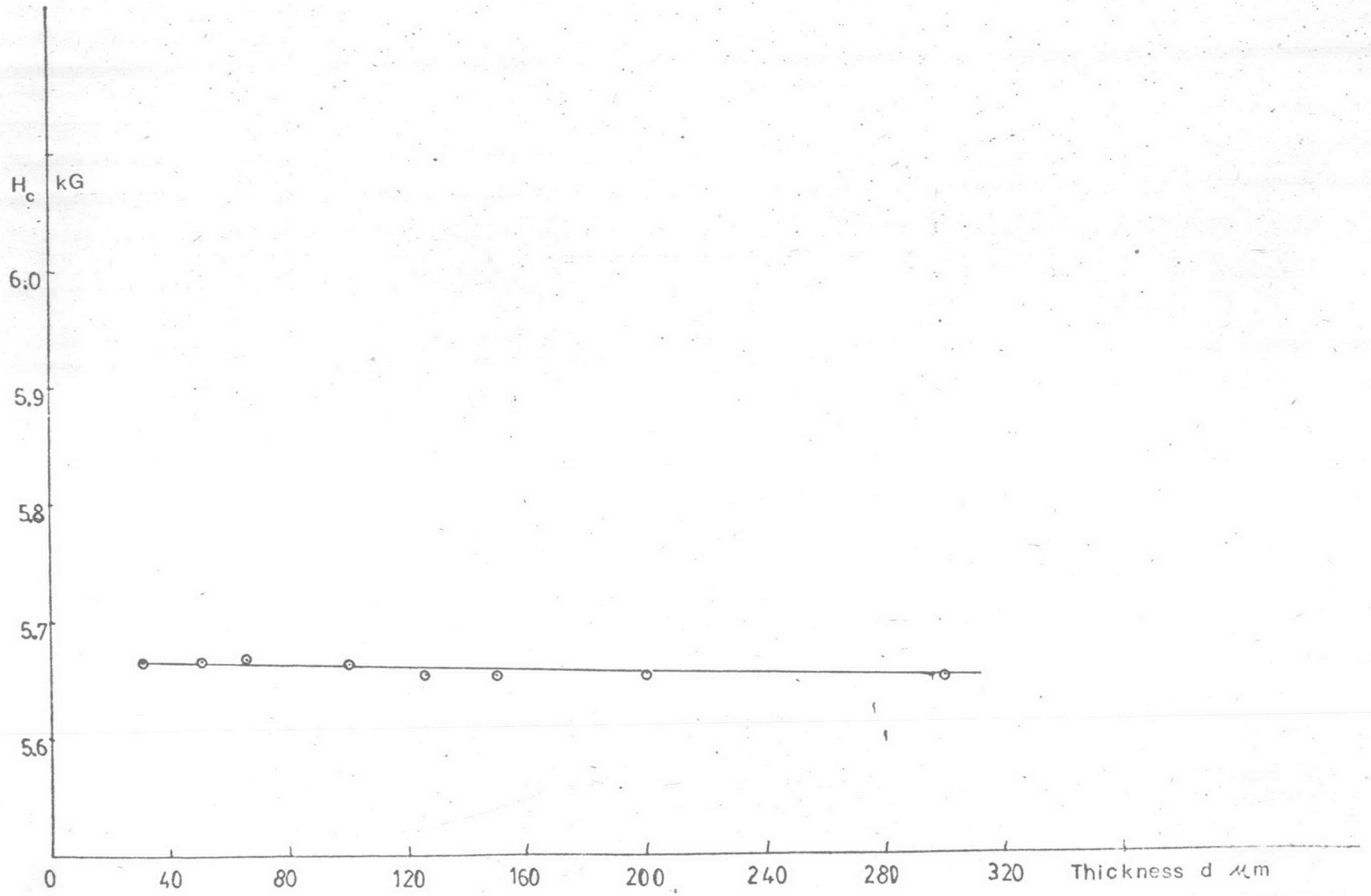

Fig. 20 Critical field dependence on sample thickness for PAA/CP with 0.5% of CP

2.3.6 Temperature dependence of the critical field

The values of the critical fields of PAA/CP systems with various concentrations of CP at different temperatures are shown in Table 4 and plotted in Fig. 21. Sample thickness was 150 μm for all samples studied.

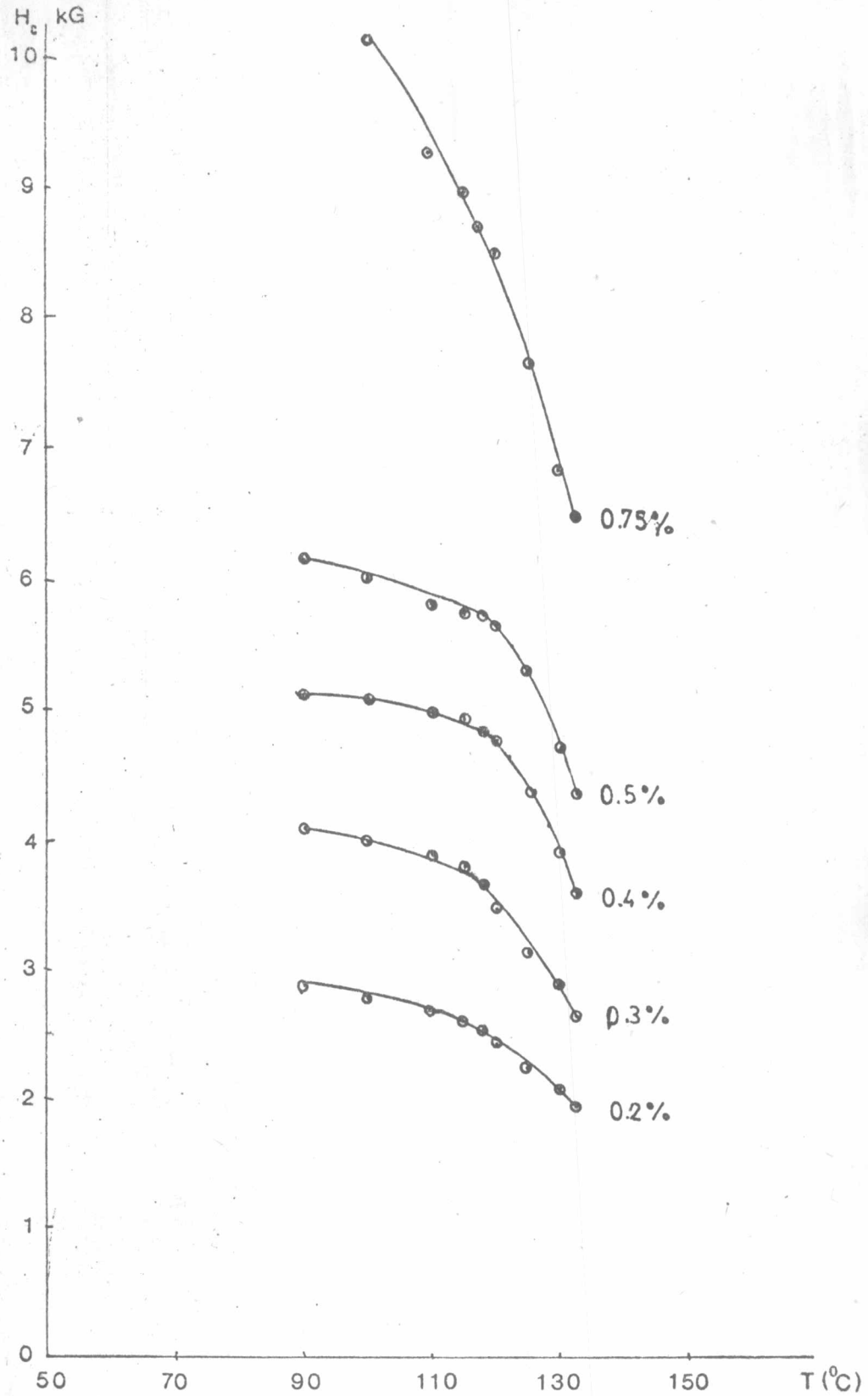

Fig. 21 Temperature dependence of the critical field for PAA/CP of various CP concentrations and sample thickness of 150 μm